The College at Brockport: State University of New York
Digital Commons @Brockport

Biology Master's Theses

Department of Biology

8-12-2012

A Study of the Sequestration of Melanin-Concentrating Hormone Receptor-1 in Caveolae: A Potential Mode of Cell Signaling Regulation by an Appetite-Stimulating Hormone

Lauren D. Field
The College at Brockport

Follow this and additional works at: http://digitalcommons.brockport.edu/bio_theses

Part of the Biology Commons

A Study of the Sequestration of Melanin-Concentrating Hormone Receptor-1 in Caveolae: A Potential Mode of Cell Signaling Regulation by an Appetite-stimulating Hormone

By

Lauren Denise Field

A thesis submitted to the Department of Biology of The College at Brockport, State University of New York, in partial fulfillment of the requirements for the degree of

Master of Biology

August 12, 2012

The College at
BROCKPORT
STATE UNIVERSITY OF NEW YORK
DEPARTMENT OF BIOLOGY

Thesis Defense

Date: 8/24/12

Committee Members	Approved	Not Approved	Comment

Laurie B Cook Major Advisor   X   ___

(signature) Committee Member   X   ___

(signature) Committee Member   X   ___

Graduate Director: _(signature)_

Department Chair: _(signature)_

Dedication

This thesis is dedicated to Mr. Simpson, without whom I never would have discovered my love for biology.

Acknowledgements

My Parents, Kim Kvocka and Brownlee Field for always being supportive and encouraging, allowing me to follow my dreams

Laurie Cook, for being the best advisor a girl could ask for, showing me how women can have a family and a career

Rey Sia and Dawn Newman, for making my teaching experience a blast, and always there to answer my questions

Danielle Feligno, Jay Moden, Bryan Pratt, Andrew Goodspeed and Christine Sharlow, for making my two years at Brockport fun and unforgettable

Table of Contents

List of Figures

Abstract

The prevalence of obesity in the United States of America has increased over the last twenty years. This prevalence has led to an increase in the study of the hormones involved control of metabolism and satiety to further understand the factors involved in obesity. One of these hormones is melanin-concentrating hormone (MCH). Many of the studies of MCH focus on the brain, while little work is done on the peripheral tissues. In adipose cells stimulation with MCH causes a release of leptin through activation of melanin-concentrating hormone receptor-1, a G-protein coupled receptor. MCHR1 becomes desensitized after activation with MCH, but the method of desensitization is unknown. ELISA studies show that internalization of the receptor is low unless proteins in the clathrin pathway are incorporated, so another method of desensitization must be occurring. Through sucrose-gradient centrifugation MCHR1 co-localizes with caveolin-1, suggesting a role for lipid rafts in receptor dynamics. This thesis will examine the extent of interaction between caveolin-1 and MCHR1. The first aim will be to determine the degree of co-localization of receptor and caveolin-1 under varying conditions. The second aim will be to analyze the dynamics of the MCHR1 within caveolae after MCH stimulation and with expression of the arrestins. The goal will be to better understand the interaction between caveolae and MCHR1 and possibly provide insight into MCHR1's mode of desensitization.

Introduction

Obesity: a Growing Epidemic in the United States

Obesity is a growing epidemic throughout the United States. According to the Center for Disease Control and Prevention (CDC), one third of all adults and a staggering 17 percent of children are obese (Flegal et al., 2010). In 1985, only 8 states had a high obesity incidence of 10 to 15 percent. Twenty-five years later, 12 states have an obesity incidence over 30 percent (Flegal, 2012). This dramatic increase is detrimental to the overall health of the nation. Overweight and obese individuals have a greater propensity to develop serious diseases, which include coronary heart disease, type 2 diabetes, hypertension, respiratory problems, various cancers and reproductive disturbances (Must, 1999; Pasquali et al., 2003).

This increase in obesity incidence has spurred numerous companies to attempt to develop an easy cure. Weight-loss pills containing stimulants and crash diet plans offer quick results with unhealthy side effects. One example of a risky diet pill is fenfluramine/phentermine (nicknamed fen/phen), which caused pulmonary hypertension and heart valve problems in users; some of these complications proved to be fatal (Berg, 1999). Healthy eating habits and exercise have shown results for those willing to do the work. But, what if an individual does put in the time and effort and a healthy lifestyle still does not work? In these cases, it is possible that hormonal imbalance is causing

decreased metabolism and weight gain. Is there a safer way of developing a drug to boost an individual's weight loss?

Hormone pathways are complex and depend on numerous inputs from the body and external feedback to maintain balance (Jehan et al., 1993; Alkemade et al., 2005; Wintermantel et al., 2006). Hormones monitor numerous functions in the body, one of which is the drive to take in food. The regulation of food intake and metabolism is complex, with numerous hormones and signaling pathways contributing to the overall process (Wang et al., 2002; Berthoud, 2008). The proteins that control hormonal pathways are broken down into four distinct subgroups: tyrosine-derivatives, steroids, peptides and proteins. While there are different types, each hormone acts basically in the same way: by attaching to a receptor and causing a cellular change within the targeted cells. As the hormones and their receptors are studied, they provide an important method of targeting diseases through treatment with hormones themselves or with receptor blockers to inhibit hormonal action.

One well-known and effective hormonal drug is the oral contraceptive pill, used by 10.7 million women in the United States (Mosher et al., 2010). Hormonal contraception works by overriding the natural cycle of hormones in a woman's body and prevents pregnancy from occurring. The main type of contraception is a combination of estrogen and progesterone that ensures no egg maturation and no ovulation (Hatcher, 1998; Rivera et al., 1999). In

contrast, examples of treatments that block receptors include α- and β-blockers, which act upon the α- and β- adrenergic receptors. These receptor agonists help to treat numerous diseases from cardiac arrhythmias and hypertension to post-traumatic stress and social anxiety disorders (Frishman et al., 2005).

Since both administration of hormones and receptor blockers have been used successfully, it is possible that there are parts of the satiety pathway that could be targeted as a treatment for obesity. There are numerous hormones involved in hunger and satiety, making targeting in this way a complex task. Understanding how each hormone that contributes to metabolism and food intake works is vital to successfully treating the growing numbers of obese individuals. This thesis will focus on one hormone in the pathway, melanin-concentrating hormone, its function and behavior within the cell membrane.

G-Protein Coupled Receptors

Many hormones utilize G protein-coupled receptors (GPCRs) for signaling. GPCRs have seven hydrophobic α-helix trans-membrane domains with an internal carboxyl-terminal end, and external amino-terminal end. They interact internally with guanine nucleotide binding proteins or G-proteins. There are numerous types of GPCR families, where the external sections of

the receptor interact with specific hormones to cause a cellular response

(Rosenbaum et al., 2009).

Internally, G-proteins function in a similar way, with signal specificity

produced by the types of G-protein subunits used (Figure 1). The G-protein is

a heterotrimer that is comprised of two protein subtypes, the α, and βγ

obligate dimer and each plays a part in the activation of the GPCR. The α-

subunit is a GTPase that acts upon guanosine diphosphate (GDP) when the

G protein is inactive. The GTP is bound to the α-subunit when the GPCR is in

a resting state (Figure 1A). After the receptor is activated through ligand

binding, the α-subunit becomes activated and releases GDP then binds to

guanosine triphosphate (GTP) (Figure 1B). The conformational change in the

α-subunit after ligand binding also causes the βγ-subunit to dissociate. After

dissociation both the α-subunit and the βγ-subunit initiate various internal

signaling cascades through interactions with effector molecules (Figure 1C).

After this interaction, the α-subunit catalyzes the hydrolysis of GTP to GDP,

which restores the association between the α-subunit and the βγ-complex

(Figure 1D). This returns the GPCR to its resting state, where it can begin the

process again if hormone is available (Boguski and McCormick, 1993).

Depending upon the type of α-subunit, the GPCR can act in many

different ways. The three well-known pathways are $G_{i/o}$, G_s and G_q and each

activates a different internal signaling pathway depending on its α-subunit

(Figure 2). The cyclic AMP (cAMP) pathway is either stimulated by G_s

Activation of G-protein Coupled Receptors
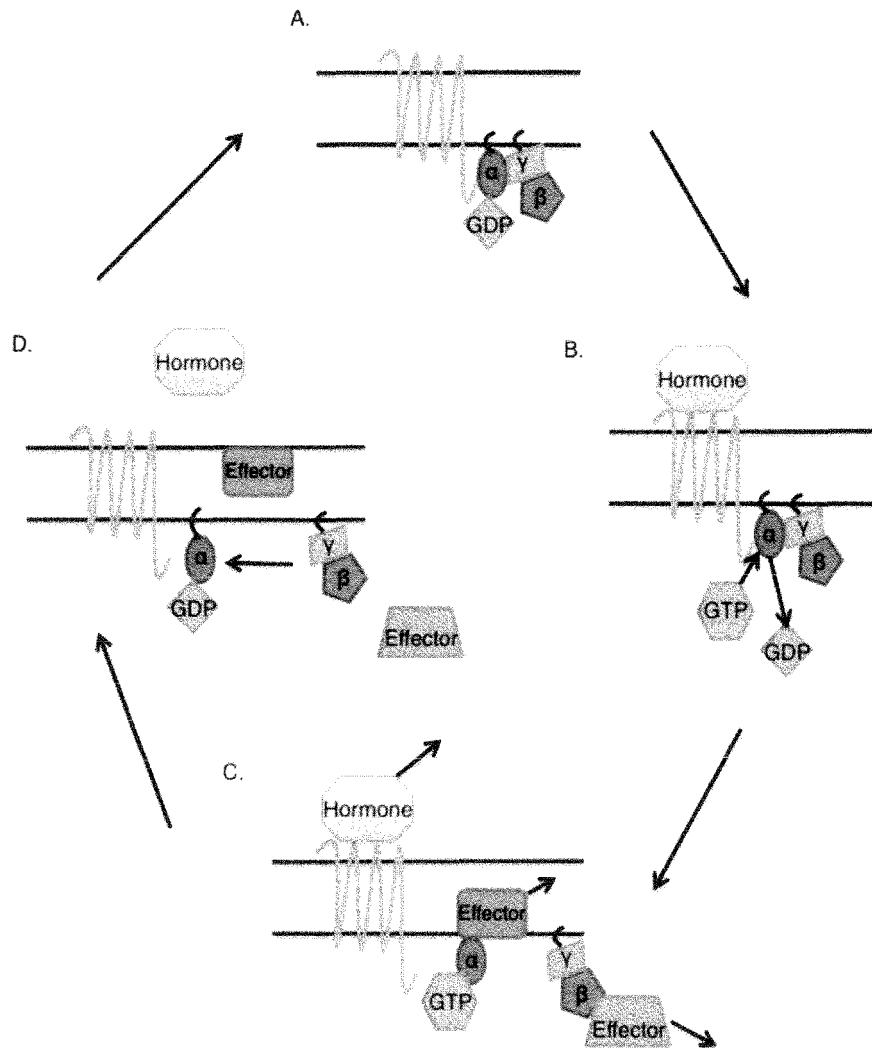
Figure 1: A) Inactivated State. **B)** Binding of hormone causes the α-subunit to exchange a GDP for a GTP. **C)** This exchange causes the α-subunit to dissociate from the βγ-subunit and each subunit interacts with an effector molecule. **D)** The α-subunit converts the GTP to GDP which allows for the two subunits to re-associate into the heterotrimer and converts the GPCR back to the resting state.

signaling or inhibited by $G_{i/o}$. Through adenylyl cyclase, these two G-proteins can change the generation of cAMP and indirectly effect the activity of protein kinase A (PKA) (Figure 2A&B). The G_q pathway works not on cAMP but uses Phospholipase C (PLC) to cleave membrane bound PIP_2 into inositol triphosphate (IP3) and diacylglycerol (DAG) (Figure 2C). Once cleaved, DAG stays in the membrane and activates Protein Kinase C (PKC) with the assistance of calcium, while the IP3 acts upon the IP3 receptors in the endoplasmic reticulum to release Ca^{2+} stored there. Finally, the G_o type of receptor also activates the PKC pathway. For both the G_q and G_o pathways, the activation of PKC causes RAS to be phosphorylated and signal to RAF and activates the MAPK pathways (Figure 2C&D) (Marinissen and Gutkind, 2001). These internal signaling cascades can cause numerous biological responses, the most common being a change in the transcription of targeted genes within the cell.

Due to the different nature of GPCR's, hormones can have both short- and long-term effects. In the short term, increases in cellular calcium can cause endocytosis of stored hormone, much like the release of thyroid-stimulating hormone (TSH) from the pituitary in response to the G_q pathway of the thyrotropin-releasing hormone (TRH) receptor. This release of TSH causes the thyroid to release thyroid hormone into the bloodstream (Blake, 1974). In the long term, cells can alter transcription due to hormone

Signaling Pathways for Gα Subgroups
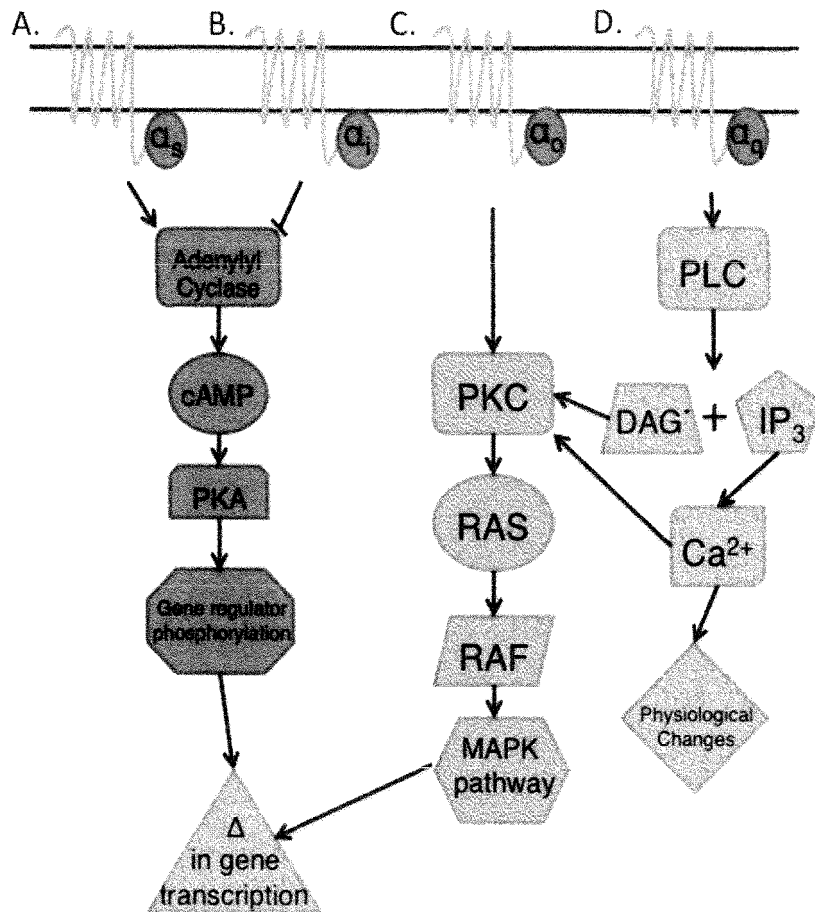
Figure 2. A) G_s stimulates the cAMP pathway. **B)** G_i inhibits the cAMP pathway. **C)** G_o activates the ERK pathway while **D)** G_q activates PLC to produce IP_3 and DAG, both of which cause changes in the ERK pathway. Most of the signaling pathways eventually change the transcription occurring within the cell. Release of calcium can cause other physiological changes.

stimulation. One example is the stimulation of the adrenal glands with adrenocorticotropic hormone (ACTH), which uses a G_s pathway to cause release of cortisol from the adrenal glands. The cortisol released causes an increase in blood sugar due to a change in the transcription of glucagon and a suppression of the immune system (Marieb and Hoehn, 2010).

The cyclic activation of a GPCR means that it can be continuously on. This continuous stimulation would be counterproductive for the cell, so there are numerous methods of terminating receptor signaling. First, having hormones that degrade allows for physical removal of the stimulus. Second, the receptor can be modified to become unresponsive. These modifications can be through phosphorylation, or ubiquination or even interactions with other molecules that can inactivate the receptor. Third, removal of the receptor from the membrane can cause desensitization, as there is no receptor to signal present on the membrane (Ferguson et al., 1998).

Clathrin-mediated Endocytosis

The most characterized pathway for receptor internalization is clathrin-mediated endocytosis. Thomas Roth and Keith Porter took the first electron micrograph images of clathrin-coated pits in 1964 (Roth and Porter, 1964). In 1975, Barbara Pearse discovered and characterized the clathrin molecule that

was the cause of the pits seen by Roth and Porter (Pearse, 1976). The basic

pathway of the clathrin-coated pit is simple: a pit (or invagination) is formed on

the surface of the membrane coated in target proteins, and then the pit is

physically removed from the membrane (Figure 3A). There are quite a few

molecules that facilitate this type of removal from the membrane. One is

clathrin, which forms a defined coat on the internal side of the invagination.

There are over fifty other proteins that can be involved in the three-step

process of internalization. The first step involves proteins that select the

membrane area targeted for internalization and facilitate the attachment of

clathrin and the coat proteins to the membrane (Traub, 2003). In the second

step, proteins are involved in attaching the internalizing vesicle to actin and

maintaining the energy dynamics needed to move the vesicle within the cell

(Qualmann et al., 1999). The proteins involved in the third step help remove

the protein coat from the clathrin-vesicle so that it can fuse with an endocytic

vesicle which will then break down the targeted molecules (Massol et al.,

2006).

To identify these endocytic vesicles, certain G-proteins, unrelated to

the heterotrimeric G-proteins previously mentioned, that are localized to

specific vesicles are targeted. For identification of clathrin-coated vesicles and

early endocytic vesicles, RAS-related protein 5 or Rab5 is used (Stenmark et

al., 1995). Late endosomes are identified by RAS-related protein 7 or Rab7

(Cantalupo et al., 2001). The proteins associated with vesicle internalization

10

Clathrin-Mediated Endocytosis and Caveolae Internalization

A.

Clathrin-
coated pit

Clathrin-
coated
vesicle

Recycling
endosome

Early
endosome

Late
endosome

Lysosome

B.

Caveolae

Caveosome

Endoplasmic
reticulum

Nucleus

✳	Clathrin
✛	RAB 5
✿	RAB 7
⬡	Caveolin
✦	Receptor
✸	SW40 virus
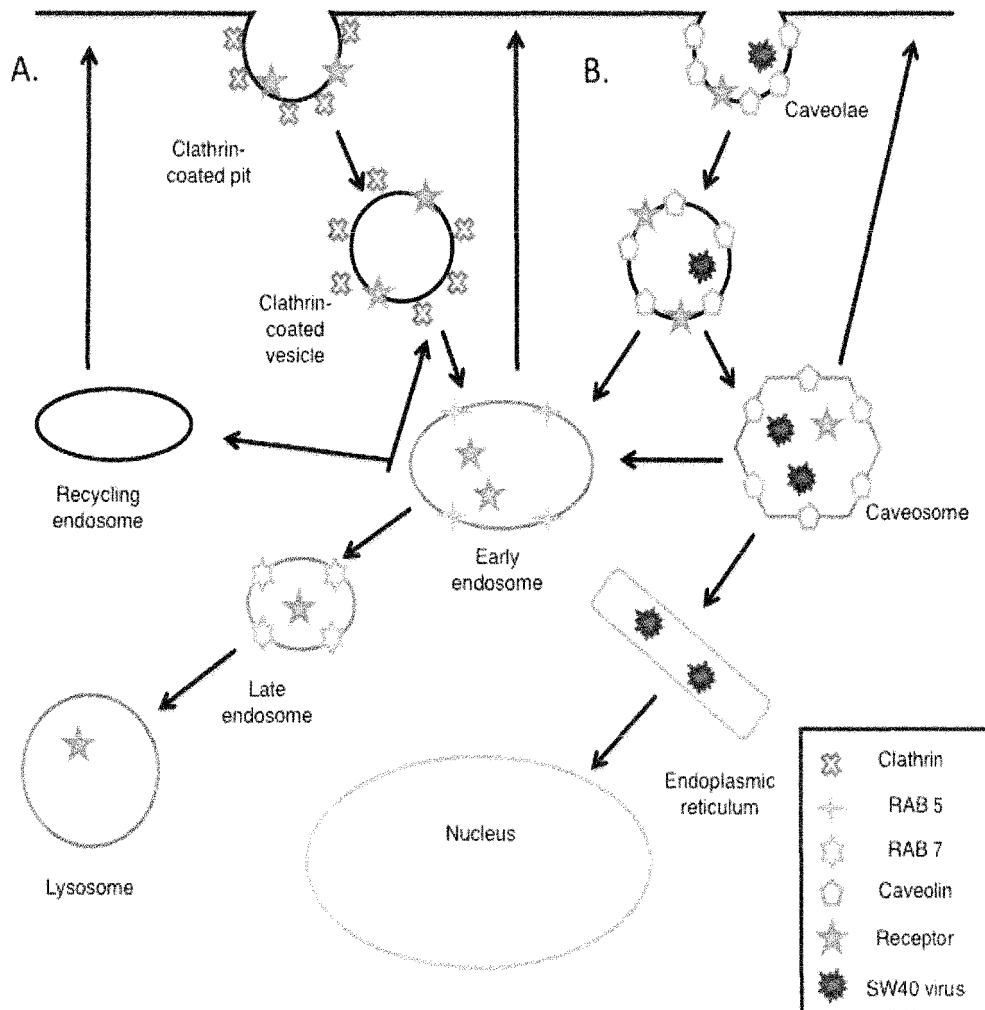
Figure 3. A) Internalization of a clathrin-coated pit, which loses the coat and then transfers its material to the early endosome, where the membrane can be recycled or sent to the late endosome. **B)** Internalization via SV40 stimulation for Caveolae. The internalized section can move to the early endosome or to the caveosome. By internalizing this way, the SV40 virus can bypass the lysosome by moving from the caveosome to the ER, as pictured. (adapted from Balklava and Grant, 2006)

11

are quite efficient, and the process of internalization can occur within a minute of the first clathrin molecule joining with the membrane. This can occur at rates of 0.35-0.45/minute—measured as the ratio of external radioactivity to internal radioactivity with iodinated EGF (Huang et al., 2004).

Two molecules that are part of the clathrin-mediated pathway are β-Arrestin 1 and β-Arrestin 2. These are proteins that are involved in alternative cargo adaption specific to internalization of certain types of receptors, such as the β_2- adrenergic receptor. They bind to phosphorylated forms of the GPCR's and uncouple them from signaling pathways (Shenoy and Lefkowitz, 2003). The two β-Arrestins help initiate the clathrin-mediated endocytic pathway that efficiently internalizes the receptor. These proteins have been more broadly linked to the facilitation of internalization of many more types of GPCR's. Interactions between the arrestins and ERK1/2 and parts of the JAK/STAT pathway help facilitate cooperation between the signaling cascades and the GPCR (Luttrell and Lefkowitz, 2002). Overall, clathrin-mediated endocytosis is a complex pathway that efficiently removes receptors from the membrane and facilitates desensitization (Oakley et al., 1999). This is not the only method of desensitization, however, and interaction of receptor with lipid rafts can affect the dynamics of the receptor's activation and desensitization (Gustavsson et al., 1999).

Lipid Rafts

Lipid rafts were first noticed in electron micrographs in the 1950's by Palade, seeing what were described as invaginations in the plasma-membrane that were 'flask-shaped' (Palade, 1953). The invaginations were distinguishable from the clathrin-coated pit because they lacked a coat molecule, and the name caveolae was adopted, which is Latin for 'little caves'. These areas on the membrane are classically lighter in density than the rest of the lipid membrane due to high levels of cholesterol and sphingolipids (Fridriksson et al., 1999). They are characterized as being detergent insoluble, and so will resist being broken down like the rest of the membrane when a non-ionic detergent is applied to cells (Brown and Rose, 1992).

There are three structural proteins, caveolin 1, 2, and 3, that are involved in maintaining the stability of caveolae on the membrane. The most prominently expressed of the three is caveolin 1, which is present in endothelial, fibrous and adipose tissues. Caveolin-1 oligomerizes to help form an invaginated structure with both the C and N termini intracellular (Parton, 1996; Smart et al., 1999). Caveolin 2 is co-expressed with caveolin 1, but the loss of caveolin 2 does not affect the formation of caveolae, whereas the loss of caveolin 1 would affect formation of caveolae (Fujimoto et al., 2000). Finally, caveolin 3 is expressed only in skeletal and smooth muscle cells. The loss of caveolin 3 causes cardiac myopathy, which indicates a regulatory or signaling role for caveolin 3. In cases where the caveolin proteins are knocked out in

mice, there is normal fetal development but a decrease in life span due to issues with angiogenic responses, hypertrophic lungs and the aforementioned cardiomyopathy (Tang et al., 1996; Figarella-Branger et al., 2003).

Caveolae and Internalization

Caveolin is synthesized as a membrane protein in the endoplasmic reticulum, is sent to the golgi and is eventually packaged into lipid rafts. It is important to note that the pool of caveolin in the golgi is detergent soluble; the insoluble nature of caveolae arises when the cholesterol, sphingolipids and caveolin complex together (Monier et al., 1995). On the membrane itself, the caveolin proteins within caveolae are immobile: fluorescence recovery after photobleaching intracellular caveolin has a high mobile fraction, but caveolin associated with the membrane has a very low mobile fraction, about 5 to 10 percent (Thomsen et al., 2002). Caveolae have been shown to internalize in response to administration of okadaic acid (a phosphatase inhibitor) and in response to infection with the Simian virus 40 (Parton et al., 1994; Pelkmans et al., 2001). After internalization, the structures remain as a stable unit, and they can either fuse with a caveosome, independently from a Rab5, or they can shuttle the membrane segment to an early endosome dependent upon Rab5. A caveosome is a large internal endosome containing caveolin-1. In either case the oligomerized caveolin can be shuttled back to the membrane, to maintain the caveolae structure (Figure 3B)(Nichols, 2003).

14

Caveolae and Signaling

Caveolae play an important function in cellular signaling. Numerous cellular receptors have been immunoprecipitated in conjunction with caveolin proteins. Certain pathways like eNOS and Src kinase are dependent on the presence of caveolins and caveolae domains for proper function (Igarashi et al., 1999). Interestingly, caveolin-1 is known to interact with Gα subunits (s,o and i), H-RAS and Src kinases, but only when they are inactive. If the receptors are mutated so that they cannot signal, they do not associate with caveolin-1. This indicates that caveolins preferentially associate with inactive receptors and are dissociated from activated receptors (Li et al., 1995, 1996; Song et al., 1996).

Caveolae, or caveolin, also interact with insulin receptors in adipocytes. In adipose tissue, insulin receptors move into and out of caveolae. The receptors move into caveolae to signal, and a decrease in signaling is seen when cholesterol is inhibited (Gustavsson et al., 1999). This means that the interaction between caveolae and the insulin receptor facilitates proper signaling for the receptor. In the cases of vascular endothelial growth factor (VEGF) and epidermal growth factor (EGF), they do not move into and out of caveolae. For these receptors, instead of a reduction in signaling due to cholesterol depletion, there is an increase in activation if caveolae domains are removed (Furuchi and Anderson, 1998; Labrecque et al., 2003).

Finally, an important function of caveolin lies in its effect on lipid regulation, through interactions with lipid molecules. There is a large amount of caveolin present in adipose tissue, with an almost a ten-fold difference between undifferentiated adipose cells and fully differentiated adipose cells (Fan et al., 1983). Adipose cell membranes are thought to be comprised of up to 40 percent caveolae domains (Parton and Simons, 2007). Caveolin has been shown to interact with cholesterol, fatty acids and lipid droplets in cell culture and in vivo (Sleer et al., 2001). It has a role in the uptake of fatty acids into the cells, along with the transport of cholesterol within the cell (Pol et al., 2001, 2004). It is possible that for different receptors, the interaction between each of the caveolae components—cholesterol, sphingolipids and caveolin—can regulate the activation of the receptor to produce the most effective signaling potential required for the cell type (Chini and Parenti, 2004).

Hormonal Regulation of Obesity: Leptin

Leptin is an adipose-derived hormone that plays a very important part in the satiety pathway. In 1994, Jeffery M. Friedman discovered that loss of functional leptin was the cause of an obese strain of mice that had developed in the Johnson Laboratory's mouse colony in the 1950's (Zhang et al., 1994). Leptin is now known to signal from the adipose tissue into the hypothalamus in the brain, crossing the blood-brain barrier (Banks et al., 1996). It acts upon

16

neuropeptide Y neurons to inhibit the release of neuropeptide Y (an appetite stimulator) and by doing so, decreases food intake (Morrison et al., 2005).

After the discovery of leptin, the obese mice in the Johnson Laboratory's colony could be classified into two different subgroups. The first is an *ob/ob* genotype that has either a loss of leptin production or a knockout of the gene and a *db/db* genotype that has a loss of function of a knockout of the leptin receptor (Drel et al., 2006). Leptin *ob/ob* knockout mice show a dramatic increase in weight compared to wild-type that is largely the result of increased adipose tissue, which is due to hypometabolic rates and hyperphagia. Leptin knockout mice also showed an insulin intolerance and a reduction in reproductive abilities, both of which have also been seen in obese individuals as mentioned previously (Berg, 1999; Pasquali et al., 2003).

After the discovery of leptin and its functional role in appetite control, it seemed that leptin might be the cure for obesity, so work was done to try to counteract the effects that leptin loss had on the *ob/ob* mice. After administration of leptin, knockout mice showed a decrease in body weight and a corresponding loss of fat tissue. They also regained their insulin sensitivity (Cohen et al., 2001). Initially, it was thought that leptin could be the much sought-after cure for obesity in humans, producing a 'magic pill' to treat obesity. Using leptin as an anti-obesity treatment, however, only worked in an extremely small number of cases, which aptly corresponded to those who had a deficiency of leptin as the cause of their obesity. Leptin was successfully

used to treat a congenital leptin deficient child; she displayed marked

hyperphagia at the age of 4 months, and at age 9 weighed 94.4 kilograms

(99.9 percentile). Two weeks after leptin administration, she started losing

weight, for a total of 15.6 kg within the year (Farooqi et al., 1999). While leptin

treatment worked in this case, it does not for the majority of the population

(Bell-Anderson K.S. and Bryson J.M., 2004).

Leptin is produced in the adipose tissue and the amount of leptin

secreted in the blood is proportional to the amount of fat that is in the body

(Klein et al., 1996). This means that obese individuals are producing more

leptin, which would be acting on the same number of receptors. Obese

individuals have a limited number of receptors available. There are also

higher quantities of leptin in obese individuals' bloodstreams compared to thin

individuals. This limits the number of available receptors to respond when

there is an increase in leptin in response to food intake, which causes the

negative feedback pathway to be less efficient, and eating continues

(Rahmouni et al., 2002). This issue can lead to an even greater increase in

weight, making correction of the imbalance important for successful weight

regulation.

Leptin has turned out to not be the magic drug that it was originally

though to be. The hormonal control of satiety is much more complex than

originally assumed, and each part of the pathway acts in a different manner.

Therefore, it is important to understand the entire feedback pathway used to

produce leptin in order to more fully treat the imbalance occurring in obese individuals. This has led to an investigation into another hormone in the satiety pathway: melanin-concentrating hormone (MCH).

Melanin-concentrating Hormone

Melanin-concentrating hormone was first discovered in Teleost fish where it concentrates melanin and causes a lightening of the scales (Kawauchi et al., 1983). When it was identified in mammals, however, it was discovered that it has little to do with melanin control and much to do with the satiety pathway (Tritos et al., 2001). Melanin-concentrating hormone is composed of 19-amino acids and forms a ring (Figure 4). A disulfide bond between two centrally placed cysteine residues (Cys7 and Cys16) defines this ring structure, which is essential for proper hormone function (Lebl et al., 1988). MCH expression is highly concentrated in the perikarya of the lateral hypothalamus and the zona incerta. Release of MCH from the perikarya can be stimulated through administration of potassium and calcium (Naito et al., 1985). Additionally, expression of the receptor is distributed throughout the body—which points to a neurotransmitter or a neuromodulator type role for the hormone (Bittencourt et al., 1992). It is possible that MCH has many functions throughout the body, in both behavioral and physical responses. Physiologically, rats with high expression of, or treated with MCH were mildly

Structure of Melanin-Concentrating Hormone

NH_3^+

CO_2^-

Asp

Phe

1

19 Val

Asp

Gln

Met

Trp

Leu

5

Cys

Arg

Cys

15 Arg

Met

Pro

Leu

Tyr

Gly

Val Arg

10
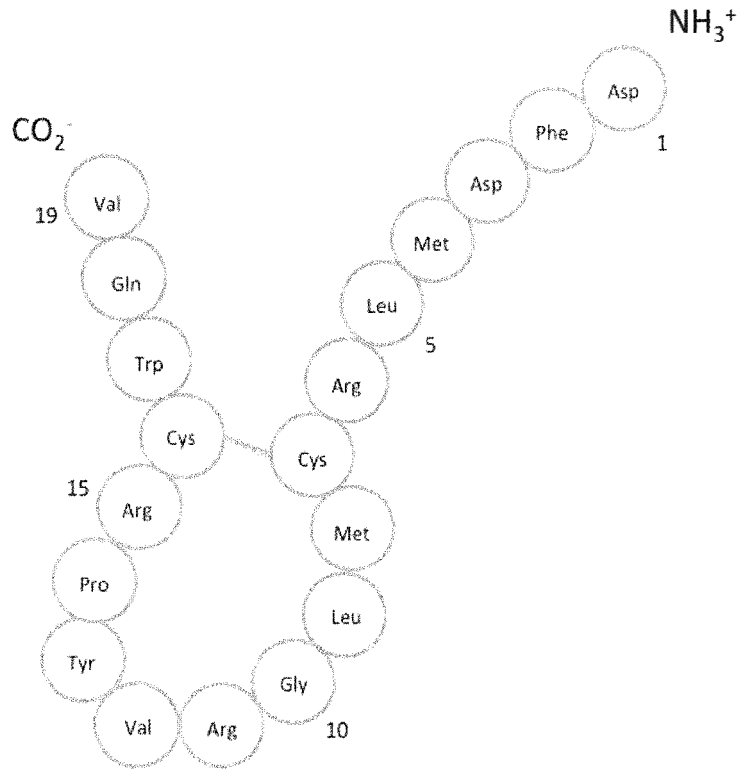
Figure 4: Melanin-concentrating hormone is a 19 amino acid peptide with a cystine bridge between Cys^7 and Cys^{16}. (adapted Pissios et al)

obese and had significant insulin resistance. Pancreatic islets were hypertrophied, indicating that MCH might be an activator of insulin production (Ludwig et al., 2001). Additionally, the receptor for MCH is found in beta-cells in the pancreas, further supporting a larger role for MCH in metabolism (Pissios et al., 2003). Treating rats with a MCH receptor inhibitor mimicked treatment with an antidepressant drug and eased social anxiety (Borowsky et al., 2002; Chen, 2002).

MCH is known to be an appetite activator, and when administered orally it causes an increase in food consumption within the hour and the effects last up to six hours (Qu et al., 1996). Mice given MCH for long periods of time show increased weight, and if there is a universal overexpression of MCH in mice obesity and insulin resistance is observed (Ludwig et al., 2001). Interestingly, leptin *ob/ob* mice show an increase in MCH expression in the hypothalamus, possibly as an attempt to signal a greater response for leptin (Figure 5). Additionally, when mice are in a fasting state they have an increase in expression of MCH. After fasting for 24 to 48 hours there is an increase in mRNA for MCH to three times normal expression rates (Bertile et al., 2003). It is possible that leptin secretion, in addition to stimulating NPY and melanocyte-stimulating hormone, also feeds back negatively upon MCH secretion, forming an efficient feedback pathway to regulate satiety control (Figure 5).

Melanin-Concentrating Hormone Feedback Pathway
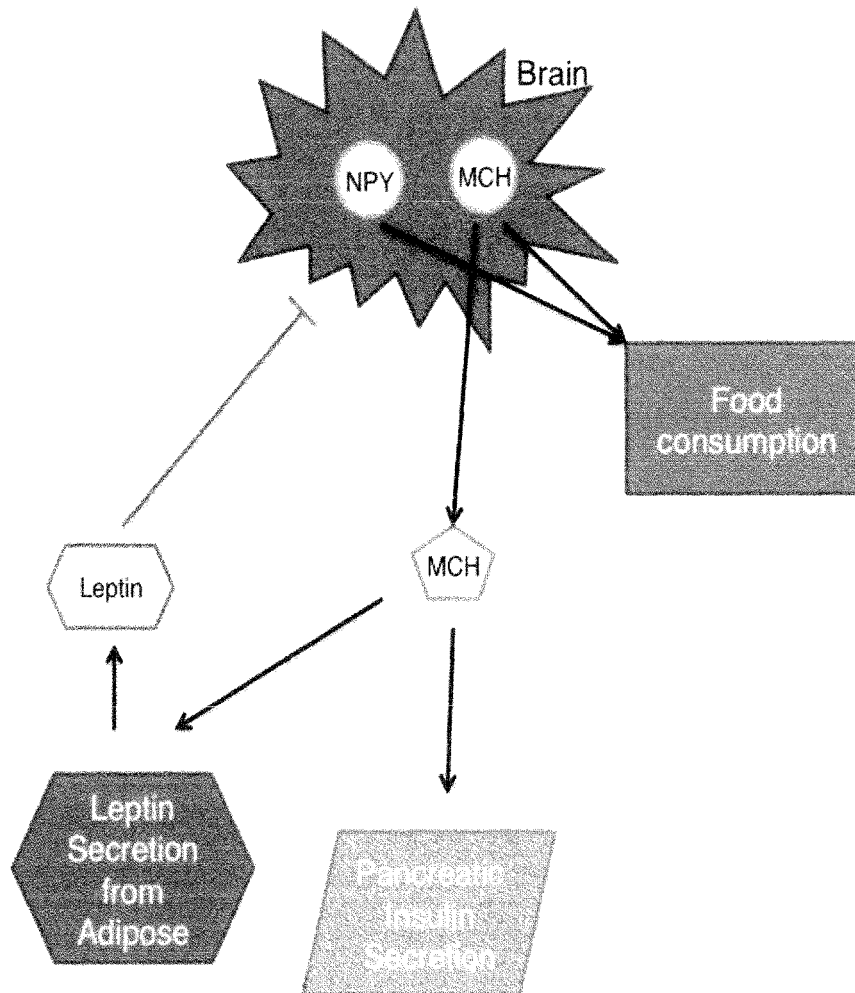
Figure 5: Neuropeptide Y and MCH neuronal stimulation increases hunger, causing an increase in food consumption. MCH is secreted and in the body, and acts upon the pancreas and adipose tissue. In adipose tissue, it causes the secretion of leptin which feeds back to the brain and causes inhibition of appetite stimulation by acting upon the NPY and MCH neurons. (adapted from Shi, 2004)

Melanin-Concentrating Hormone Plays a Role in Appetite

When MCH is knocked out in mice, there is a lean phenotype observed due to hypophagia and a corresponding hypermetabolic rate (Tritos et al., 1998). When the receptor for MCH is knocked out in mice, a lean phenotype is also observed and the mice are also resistant to diet-induced obesity. These knockout mice display hyperphagic and hypermetobolic symptoms (Chen, 2002). Work done on an antagonist for MCH receptor has shown that when antagonist is administered over a long period of time there is a dramatic decrease in the weight of diet-induced obese mice (Takekawa et al., 2002). This supports a role for MCH in the regulation of metabolism despite food intake. If this could be successfully applied in humans, it could effectively help obese individuals lose weight without serious side effects like the cardiac complications seen after use of fen-phen (Berg, 1999). There are two receptors for MCH, the first is present in all mammals while the second is found in only dogs and primates (Tan et al., 2002).

Melanin-Concentrating Hormone Receptors

The original MCH receptor was an 'orphan' receptor dubbed SLC1/GPR24, which was identified as the specific GPCR for MCH, and was called MCHR1 (Chambers, 1999; Lembo, 1999). MCHR1 is present in all mammals, with human MCHR1 being highly homologous with rodent MCHR1,

with a protein BLAST relationship of 96% identities and 98% positives, meaning that 98% of the amino acids in each protein have the same functionality, and 96% are exactly the same (Blast1). After the discovery of MCHR1, it was determined that humans have a second MCH receptor which shares sequence homology with the core of MCHR1 (Hill et al., 2001; Mori et al., 2001). Comparing the human MCHR1 with MCHR2, a protein BLAST showed that MCHR2 is comparable to 70% of MCHR1, with 37% identities within that region and 57% positives (Blast 2).

Studies done in rats show that the MCHR1 acts as both a G_i- and a G_q-coupled receptor. Stimulated cAMP was suppressed and a change was seen in intracellular calcium levels, both of which were caused by MCHR1 activation (Hawes et al., 2000; Pissios et al., 2003). In contrast, MCHR2 is thought to be exclusively coupled to the G_q pathway (Hill et al., 2001; Rodriguez et al., 2001). As there are numerous tissues that MCH acts upon, from adipose to neural tissue, it is quite possible that this stimulation causes different effects on each tissue type, as it could activate different transcriptional and cellular changes in each type of cell.

The majority of work performed studying MCHR1 has been performed in the brain. Effects of MCH include mood control and regulation of the voiding-reflex (Borowsky et al., 2002; Hegde et al., 2009). Very little work has been done to examine the effects of MCH on the peripheral tissues in the body. As mentioned previously, there are MCHR1 receptors in β-cells in the

pancreas, and MCH treatment of those cells may cause changes in insulin

production (Pissios et al., 2003). Little is known about how MCH enters the

blood, if it can cross the blood-brain barrier, or if it is produced from another

source in the body.

Desensitization to Melanin-Concentrating Hormone

MCH causes a release of leptin in adipose tissue. Having a high level

of leptin in the bloodstream reduces the ability to sense, in the brain, an

increase caused by food consumption. Adipose cells would need to become

unresponsive to MCH after the initial release of leptin to reduce the amount of

leptin produced. As stated previously, there are a few methods that a cell can

use to keep a receptor from continuously activating. These include: 1)

degradation of hormone, 2) conformationally changing the receptor through

modification or interaction with another protein, and 3) physical removal of the

receptor from the membrane. G-protein receptor kinases, or GRK's,

specifically phosphorylate the substrate bound form of the receptor. This

phosphorylation increases affinity for inhibitory proteins, or arrestins, which

inhibits further signaling by the receptor (Lefkowitz and Freedman, 1996).

Additionally, interactions between GPCR's and regulators of G protein-

signaling (RGS) cause a decrease in the activation of the receptor by

essentially increasing the rate of GTP to GDP conversion by the G protein (De

Vries et al., 2000). Interactions between specific RGS's and MCHR1 have

been identified, and may also play a role in receptor desensitization. Specifically, RGS2 causes MCHR1 inhibition of the $G\alpha_q$ pathway and RGS8 causes inhibition of the $G\alpha_{i/o}$ and $G\alpha_q$ pathways (Miyamoto-Matsubara et al., 2010). There has been work done that has shown internalization of receptor after stimulation with MCH (Saito et al., 2004; Miyamoto-Matsubara et al., 2010). It was also shown that if clathrin-mediated endocytosis was inhibited, there was only partial inhibition of endocytosis, pointing to an alternative method of internalization (Saito et al., 2004). What is unclear, however, is the length of time MCHR1 is desensitized, and if endocytosis is truly the cause of desensitization, or if there is more involved in the process.

Recent Advances in MCHR1 Signaling

MCH causes a release of leptin from adipose cells, and as there is desensitization to the hormone over a period of time, it needs to be determined which of the possible mechanisms is causing desensitization. Desensitization work being done by our lab has shown that after an initial increase in activated ERK in response to treatment, there is not a similar response seen after a second treatment was administered thirty minutes later. As stated previously, work done by Saito *et al.* has shown that in response to MCH treatment, there is an internalization of the receptor via the clathrin-mediated endocytosis pathway. They determined that there was internalization of 21.9% seen in as little as five minutes, and a greater

internalization rate of 44.2% seen after 30 minutes of treatment (Saito et al.,

2004). Attempts by our lab to replicate their internalization process have

shown that internalization of receptor without overexpression of components

in the clathrin pathway only occurs at 15 percent (Moden, 2012). This is

contradictory, and may be because of the addition of arrestins and GRKs by

Saito. If these parts of the clathrin pathway are not overexpressed, then our

work shows that there is not a high level of internalization. Tetsuka *et al.* also

looked at mutations in the C-tail of the receptor and the effect of these

mutations on activation. They found that if certain phosphorylation sites

(Arg319 or Lys420) on the tail were mutated, cellular signaling was attenuated

(Tetsuka et al., 2004).

Work performed by our lab showed that if one of the Arrestins (β1 or

β2) is co-expressed with the receptor, the internalization rate increases

dramatically up to 40 percent (Moden, 2012). This points to an inefficient

method of internalization via the clathrin-mediated endocytosis pathway. This

leads to the hypothesis that clathrin-mediated endocytosis is not the way that

desensitization to MCH is occurring. If the cells were using clathrin-mediated

endocytosis only to desensitize MCHR1, it would be expected that without

transfection of other proteins in the pathway, a significant amount of receptor

would be removed from the membrane in direct response to hormone

treatment. As mentioned previously, internalization can still occur if the

clathrin pathway is inhibited.

So, caveolins could be interacting with MCHR1 to desensitize signaling. This was substantiated by Cook *et al.* through isolation of lipid rafts via sucrose gradient centrifugation. They showed that caveolin-1 and MCHR1 are co-localized within the lipid raft fractions. Additionally, MCHR1 immunoprecipitates with caveolin-1, suggesting that caveolin-1 complexes with MCHR1 within the cell (Cook et al., 2008). This interaction could be influencing the desensitization of MCHR1 after MCH treatment. Insulin receptors move into caveolae to facilitate efficient signaling, so it seems that MCHR1 could be using some sort of version of this to change its signaling reactivity (Gustavsson et al., 1999). Also, the receptor could be moving into the caveosome after activation at a lower rate than would be seen if the clathrin pathway was being used. The method of MCHR1 desensitization is unclear, and this thesis will attempt to answer some of these questions.

Specific Aim 1

Localization of MCHR1 within caveolae has been shown by Cook *et al.* in CHO cells (Cook et al., 2008). However, the isolations were performed in a singular cell type, with one method of isolation and utilizing an epitope tag to blot for the receptor. Modifying any of these parameters could cause the receptor location to change, although it is hypothesized that the interaction between MCHR1 and caveolin-1 will be seen regardless of isolation

conditions. To further study this hypothesis, the following experiments were designed:

1. *Multiple cell types will be examined to determine if lipid raft isolation with MCHR1 co-localization can be reproduced.*

2. *The method of raft extraction will be examined through use of multiple lysing solutions with varying mechanisms for membrane perforation.*

3. *Finally, the possibility that the epitope tag is influencing receptor localization will be addressed through isolation of the wild-type receptor.*

Specific Aim 2

The dynamics of MCHR1 signaling and desensitization is still unclear. There are conflicting reports of the level of receptor internalization in response to agonist treatment, with prior work showing internalization occurs in small amounts (Moden, 2012). Addition of arrestins increases the amount of internalization, but they are highly expressed. It is hypothesized that there is very little internalization of the receptor. Additionally, the localization of receptor within caveolae may change in response to agonist administration or with the addition of the arrestins. The following experiments were devised to determine the validity of these hypotheses:

1. Visualization of internalization of receptor will be attempted without the addition of the arrestins or GRKs to support the ELISA data showing low internalization.

2. Localization of the receptor on a sucrose gradient isolation will be examined before and after agonist administration to determine if receptor location within lipid rafts changes.

3. The effect of addition of the arrestins will be determined through gradient isolations incorporating each arrestin individually to determine if the addition causes a change in receptor localization on the membrane.

Materials & Methods

Cell Culture

Cell Lines and Passaging

Three cell lines were used for this study. The first were CHO-K1 cells, or Chinese Hamster Ovary cells (ATCC), stably transfected with VSVg-MCHR1 by Laurie B Cook. These cells were grown in F12K media (CellGro) containing 5% FBS (Atlanta Biological). The second cell line was Baby Hamster Kidney (ATCC) cells grown in DMEM (CellGro) and 10% FBS. Finally the last cell line was a pre-adipocyte 3T3L1 cell line grown in DMEM+10% BCS (Atlanta Biological). All cells were passaged using trypsin EDTA (Thermo Scientific) and were passaged at 80-90% confluence for BHK and CHO lines and 50% confluence for 3T3-L1s. All cells were incubated at 37^0 C, 90% humidity, and with 5% CO_2 maintained continuously.

Differentiation of 3T3L1s

To differentiate 3T3L1s into full adipocytes, the cells were plated on 10cm dishes and allowed to grow to 80% confluency, with the media being changed as needed. On day 0 of differentiation, the cells were given DMEM+10%FBS +5% Penicillin/streptomycin (CellGro) containing 1:100 Methlyisobutylxanthine (11.5mg/ml) (Acros Organix), 1:1000 Dexamethasone (0.4 mg/ml) (Sigma) and 1:100 Insulin (1mg/ml) for a final concentration of 10 μg/ml (Sigma). On day 2 of differentiation, the cells were given DMEM+10%FBS +5% Pen/strep containing 1:100 Insulin, and on day 4 the

cells were given DMEM+10%FBS +5% Pen/strep containing 1:400 Insulin for

a final concentration of 4 μg/ml. On day 6 of differentiation, the cells were

given DMEM+10%FBS +5% Pen/strep and allowed to grow until day 10 when

differentiation was complete.

Cellular Transfection

To insert desired DNA into the CHO-K1 and BHK-570 cell lines,

LipoD293 (SignaGen) was used. The protocol recommended by SignaGen

was followed, the media was changed 24 hours post transfection and

experiments were run 48 hours post transfection. DNA concentrations for

each of the plasmids used was 1μg/ml.

Fluorescent Microscopic Analysis

Immunocytochemistry

Cells were plated on glass cover slips, and transfected with VSVg-

MCHR1 (From G.Milligan). After complete transfection 48 hours later, the

cells were treated with Melanin-concentrating Hormone (American Peptide).

To do this the media was aspirated off and one ml of DMEM- was added to

each dish. After an hour the DMEM- was removed and one ml of 1μm MCH

solution was added to the dishes, which were allowed to sit for the desired

time. The control plates were given new DMEM- instead of the MCH solution.

The cells on cover slips were put on ice and the media aspirated. The cells

were washed twice with 2 ml of cold Phosphate Buffered Saline (PBS), treated with one ml of 4% Paraformaldehyde for 10 minutes in PBS then washed three times with cold PBS.

Humidifying chambers were made using glass Petri dishes, parafilm and damp paper towels. The cover slips were moved to the humidifying chamber and 250 µl of blocking buffer (of PBS with 0.1% Triton (BioReagents) and 5% Goat Serum) was added drop-wise to each cover slip. The coverslips were incubated for one hour, and then 250 µl primary antibody, rabbit VSVg-MCHR1 (Sigma) at 1:1000 concentration or mouse RAB7 (BD Biosciences) at 1:1000 concentration in blocking buffer was added to each cover slip and allowed to sit overnight at 4^0 C. After incubation, the solution was removed and the cover slips replaced in their dishes. Each cover slip was washed for five minutes with PBS a total of three times and rocked on an orbital shaker for the duration. The cover slips were then placed back in the humidifying chambers and 250 µl of secondary antibody, goat anti rabbit AlexaFluor 488 (Invitrogen) at a 1:5000 ratio, rabbit anti goat AlexaFluor 594 (Invitrogen), and DAPI (1.0µg/ml, Roche) at a 1:5000 ratio, in blocking buffer was added to each cover slip and allowed to incubate for 45 minutes. The solution was removed and the slides transferred back to the dishes, and washed again for five minutes with PBS a total of three times on the orbital shaker.

The finished cover slips were mounted on slides using Prolong Gold (Invitrogen) and clear nail polish was used to affix them to the slides.

Microscopy

Fluorescent microscopy was performed using a Zeiss Axiocam MRm fluorescence microscope with AxioVision imaging software. Image formatting was performed in Adobe Photoshop and assembled into figures in Microsoft PowerPoint.

Cell Lysis for Caveolae Isolation

Lysing

For each gradient, two 10cm dishes of the desired cell line were grown to a confluency of at least 80%, treated with 1 μM MCH for the desired time points, and then placed on ice. Each was quickly washed twice using 5 ml of cold PBS. Three different lysing solutions were used:

1. *Basic pH 11 Procedure*: lysate is produced using 2 ml of 500 mM Na_2CO_3 at a pH of 11.

2. *Neutral pH 7 Procedure*: lysate is produced using 2ml of 25mM TRIS and 250mM sucrose.

3. *Triton Procedure*: lysate is produced using 2ml of MBS with 1% Triton at a cold temperature.

34

After the addition of the lysing solution to one of the two dishes, the cells were scraped off the dish using a squeegee, and the liquid transferred to the next dish. The scraping procedure was repeated for the second dish and then the solution was placed in a 7ml dounce homogenizer that had been chilled on ice, and 1:1000 of protease inhibitor (Sigma) was added to each homogenizer. This solution was left to swell for 30 minutes. After swelling, the solution was homogenized 10 times and allowed to swell for two minutes, after which this process was repeated 3 more times, for a total of 40 strokes.

To the bottom of an ultracentrifuge tube (Beckman), two ml of the lysate was added, along with a 90% sucrose solution made in MES buffered saline (MBS; pH6.5, 25 mM Mes, 0.15 M NaCl). The tubes were then vortexed to thoroughly mix the lysate and the sucrose solution, making a 45% sucrose layer. To the top of this layer, 4 ml of 35% sucrose in MBS with 250mM Na_2CO_3 was carefully added. On top of the 35% sucrose layer, 4 ml of 5% sucrose in MBS with 250mM Na_2CO_3 was added–ensuring no disturbance to the layer. Using a scale, two gradients were balanced to each other. The gradients were then placed on the SW41 rotor, and ultra-centrifuged for 18 hours at 4° C at a speed of 39,000 rpm. The day after centrifugation, the tubes were removed from the buckets and one ml fractions were taken from the gradient, for a total of twelve fractions. The fractions were pulled from the top of the gradient right at the meniscus. The fractions were placed in microfuge tubes and frozen at -20^0C.

SDS-PAGE

Gel Preparation

SDS-PAGE gels were made according to the following chart.

Table 1: Running Gel Recipes

Running Gels		
	10% Gel	12% Gel
40% Bis-Acrylamide	2.5 mL	3.0 mL
4X Tris-HCl /SDS pH 8.8	2.5 mL	2.5 mL
10% APS	33 μL	33 μL
dH2O	5.0 mL	4.46 mL
TEMED	6.6 μL	6.6 μL

Table 2: Stacking Gel Recipes

Stacking Gel	
	4% Gel
40% Bis-Acrylamide	488 μL
4X Tris-HCl /SDS pH 6.8	1.25 mL
10% APS	25 μL
dH2O	3.21 mL
TEMED	5.0 μL

The desired fractions were removed from the freezer and allowed to thaw. From each sample, 100 μl was added to a new microfuge tube, and to each was added 25 μl of 5X Lamelli sample Buffer. The tubes were placed in a circular rack with caps placed on top and boiled for 2 minutes. They were removed and centrifuged at 13000 rpm for five minutes. The gels were placed

in the running apparatus and it was filled with 1X Running Buffer. To the first well, 5 µl of EZRun™ pre-stained *rec* protein ladder (Fisher) was added and then the samples were added subsequently. For the 12% gels, there was 5 µl of sample loaded to blot for Caveolin-1 and to the 10% gels; 15 µl of sample was loaded to blot for the VSVg-MCHR1 or MCHR1. After the samples were loaded, the gels were run at 100 V for about 70 minutes, or until the sample buffer reached the bottom of the gel.

Semi-Dry Transfer

After the gels were run, they were removed and placed in Towbins buffer (Appendix 1) for 10 minutes. Along with the blot, two sponges (BioRad) and a nitrocellulose membrane (BioRad) of the same size were incubated. After incubation, the semi-dry transfer apparatus was set up so a sponge was on the bottom, followed by the membrane then the gel and then the final sponge. The top plate was placed over this, ensuring no bubbles and complete contact. The transfer was run at approximately 16V for 30 minutes, or until the ladder was no longer visible on the gel.

Western Blot

After the transfer, the nitrocellulose paper was placed in 5% Milk in TBS-T (Appendix 1). This blocking step occurred for 60 minutes, and after incubation 10 ml of primary antibody in TBS-T was added for each specific blot. For both Caveolin-1 (BD Biosciences) and VSVg (Sigma), the primary antibody was made at a concentration of 1:2000 in 5% milk in TBS-T. The

37

blots were allowed to incubate in primary antibody overnight. The blots were washed three times for five minutes in TBS-T. After washing, the blots were incubated for one hour in secondary antibodies, both in goat-anti rabbit HRP (BioRad) conjugated at a concentration of 1:5,000. The blots were then washed three times for five minutes each in TBS-T to remove excess secondary. A 1:1 ratio from a Western Lightning™ Chemiluminescence Reagent Plus kit (Perkin Elmer) was used; the blots were incubated for one minute in the solution, wrapped in saran-wrap and taken to the dark room. The film (Kodak) was exposed to the blots for a range of times to achieve the best exposure, then developed (Kodak) for 30 seconds, fixed (Kodak) for a minute and then dried thoroughly.

Bradford Analysis

For each gradient, Bradford analysis was performed. In a 96-well plate, a standard curve was prepared with 20 µl Bovine Serum Albumin (BSA) (0-100 µg) (Fisher Biotech). To each well, 20 µl of each sample was added, and to all of the wells, 200 µl of the Bradford solution was added. The entire experiment was run in duplicate, and the plate was read at 595 nm on the BioTek Synergy™ H1 Hybrid Reader plate reader and Gen 5 1.11 Software.

Densitometry

Using Adobe Photoshop, the desired blots were scanned in, converted to grayscale and inverted. The density was measured with a background reading used as the baseline.

Results

Lipid raft isolation using CHO cells

To determine possible changes of gradients performed in different cell types, a gradient was produced from Chinese Hamster Ovary cells. Chinese Hamster Ovary cells that had previously been stably transfected with VSVg-MCHR1 by Laurie B. Cook were lysed and a sucrose gradient was performed using a detergent-free isolation method with a pH of 11, as previously published (Cook et al., 2008). The isolated fractions were run on a 12% SDS-PAGE gel and after transferring the proteins on the gel to nitrocellulose paper, the nitrocellulose was cut below the 40-kDa molecular weight marker. A western blot was then performed on each half of the membrane, the top half was blotted for VSVg-MCHR1 and the bottom half for caveolin-1 (Figure 6).

The α-VSVg blot showed bands localized to fractions 4, 5 and 6 at the molecular weight of approximately 55 kDa (Figure 6A). The band at fraction 4 contains the highest density of protein compared to the other two bands. For the α-caveolin-1 western blot, there was a large quantity of caveolin seen in fractions 4, 5, and 6 with a molecular weight of approximately 24 kDa (Figure 6B). The caveolin in fractions 4 and 5 has a higher molecular weight band nearer to 50 kDa, possibly representing an oligomerized set of caveolin with the lipid raft. There was a smaller amount of caveolin present in fractions 3, 7-
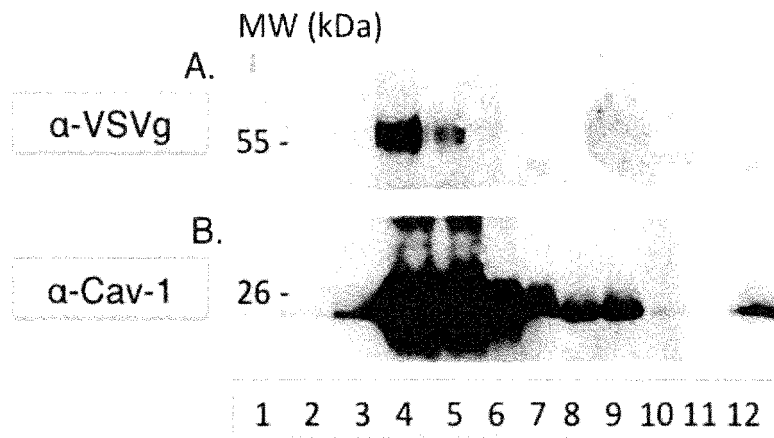
39

Figure 6: Lipid rafts were isolated using the basic pH isolation method from stably transfected CHO-K1 cells and fractions were run on a 10% SDS gel. The gel was loaded with 15 µL of sample. The gel was cut and the bottom blotted for for **A)** VSVg-MCHR1 at a 1:2000 antibody concentration and **B)** Caveolin 1 at 1:2000 antibody concentration and the top.

9 and 12. The localization of caveolin-1 and MCHR1 to fractions 4 and 5 is consistent with the previously published work, performed in this lab (Cook et al., 2008).

Isolation of lipid rafts using alternative lysing methods

While the detergent-free basic pH isolation method has been successful in isolating caveolae and has shown a co-localization between caveolae and MCHR1, there are other methods of isolating caveolae from the lipid membrane (Hooper, 1999). If only one method is examined, such as the previously described basic pH method, there is a possibility that the lysing solution, specifically the high pH, is the cause of the co-localization between receptor and lipid raft. Therefore, multiple methods were examined to verify that the isolation method does not affect localization of receptor on the gradient. To do this, current literature was reviewed and two other lysing methods were discovered. The first involved a lysing solution that contained 1% Triton in MBS performed at 4^0C, utilizing the non-ionic detergent to lyse the cellular membranes. The second contained 250mM Sucrose in a TRIS buffer—using a slight osmotic gradient to help lyse the cells (Liu et al., 1998).

The TritonX-100 method was used because lipid rafts are known to be non-ionic detergent insoluble at very cold temperatures, so they will remain structurally intact after isolation (Macdonald and Pike, 2005). The second was used as a simple membrane disruptor, with the lipid rafts being held intact by high density of lightweight lipids, and it has been proposed that the

41

glycosphingolipids form hydrogen bonds to further stabilize the membrane (Anderson, 1998). These two experiments were performed using the transfected Baby Hamster Kidney (BHK) cell model, to obtain a high level of VSVg-MCHR1 within the cells. If MCHR1 is truly localized within caveolae, then the isolation method will not change the co-localization.

The gradients were performed for each method, and twelve fractions were isolated. Lysate from each of the gradients was also kept to determine overall protein concentration from the lysing of the cells. The fractions were run on 10% SDS-PAGE gels to determine the distribution of receptor, and on 12% SDS-PAGE gels to determine the distribution of caveolin 1. The two different densities were used to ensure that the smaller caveolin molecule did not run off of the gel, and so that both gels could be run at the same rate. Additionally, by not cutting the blot, all of the available protein could be visualized.

The corresponding blots were treated with either α-VSVg antibody or α-caveolin 1 antibody. In both of the new isolation methods, distribution of caveolin is less localized than when using the basic pH detergent-free isolation method (Figure 7A&B). In both cases, instead of having a large amount of caveolin in fractions 4-6, as seen in the CHO isolation (Figure 6B), there is caveolin present from fraction 4 to the bottom of the gradient. For the neutral isolation, there is a slight increase in the density of the bands for fractions 4 and 5. The distribution of the receptor changed as well, with more

Verification of Co- Localization of MCHR1 in Caveolae
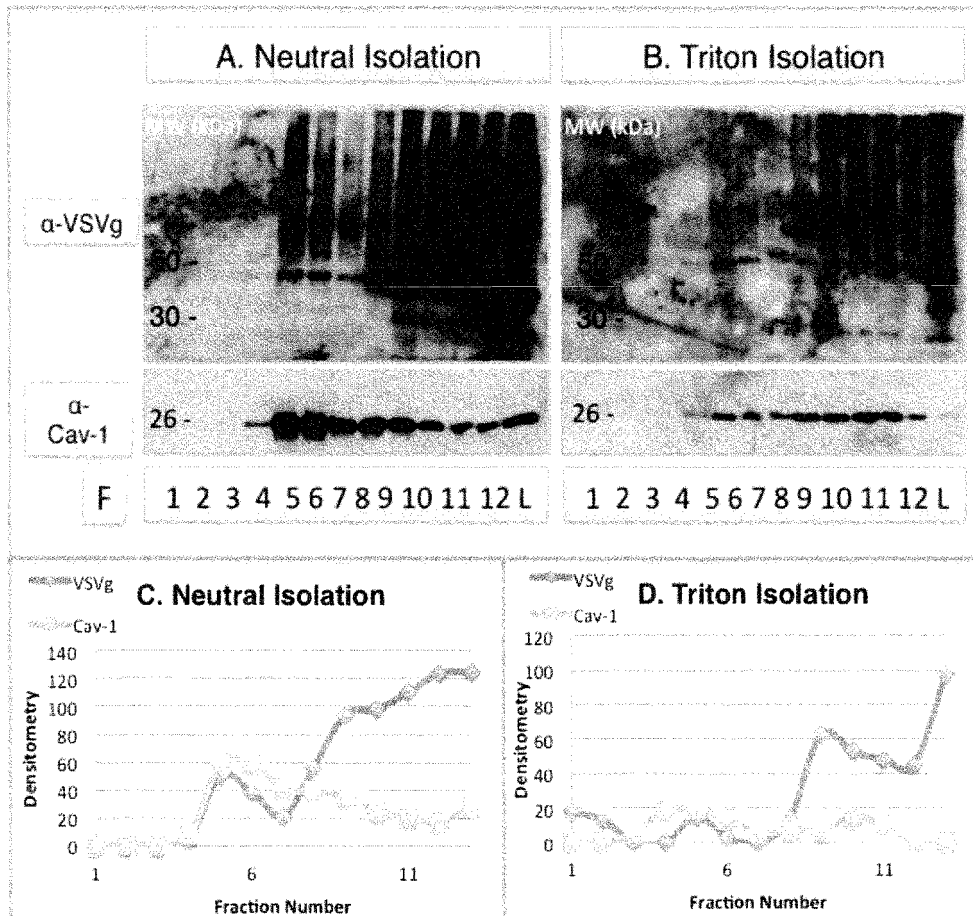
Figure 7: BHK-570 cells were transfected with VSVg-tagged MCHR1 provided by G. Milligan. The VSVg-MCHR1 blots were labeled with a 1:2000 concentration of rabbit anti VSVg antibody, while the Caveolin-1 blots were labeled with a 1:2000 concentration of rabbit anti Caveolin-1.
A. Isolation of Cav-1 using a neutral MBS solution containing 250 mM sucrose
B. Isolation of Cav-1 using 1% Triton solution in MBS
C. Densitometry analysis of Neutral Caveolin isolation
D. Densitometry analysis of Triton Caveolin isolation

of VSVg-MCHR1 present at the bottom of the gradient (Figure 7A&B). The band weights for VSVg also changed, with a band at approximately 48 kDa present in fractions 4 and 5, and large molecular weight bands corresponding to a 75-80 kDa which could possibly be a dimerized version of the receptor. In fractions 10-12, there are lower weight bands around 30 kDa that could correspond to a cleaved form of MCHR1 within the cell.

Interestingly, the density of the VSVg-MCHR1 blot follows the distribution seen in the caveolin-1 blots, even appearing to be in a density proportional to the amount of caveolin. This supports the previously published results by our lab, where there is a co-localization between caveolin-1 location and VSVg-MCHR1 location (Cook et al., 2008). To analyze this association, densitometry was performed that showed corresponding increases and decreases in the density of the fractions when comparing caveolin to MCHR1 (Figure 7C&D). Bradford analysis of both of the gradients shows that there is little overall protein at the top of the gradients, and that at fraction 5 there is an increase in protein, which increases again at fraction 9 and continues to the bottom of both gradients (Figure 8).

This relationship supports the hypothesis that there is an interaction between caveolin-1 and MCHR1. While these methods of isolation are not as successful in isolating lipid rafts as the basic pH isolation method, they do show a correlation between the presence of caveolin 1 and VSVg-MCHR1.

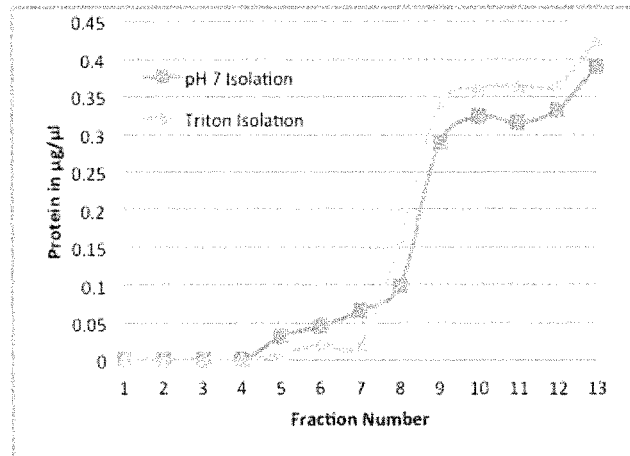**Bradford Analysis of Lysing Isolations**

Figure 8: BHK-570 cells were transfected with VSVg-MCHR1 provided by G. Milligan, and lipid rafts were isolated (Figure 7). A Bradford analysis was run on all three isolations and the fraction number was plotted against the calculated protein amount in µg/µL.

For this reason, the lysing procedure that used the detergent-free basic pH solution was used in future experiments.

Distribution of MCHR1 without an Epitope Tag

In order to continue to determine the effect of co-localization of MCHR1 to caveolae, the receptor was studied without the VSVg epitope tag. While it is easier to blot for the receptor with the epitope tag, it could influence the placement of receptor on the membrane. Adding an epitope tag to a targeted molecule allows for easy targeting of the desired protein. Antibody quality and purity are better for epitope tags, as they are used quite often to label proteins that lack quality antibodies. To complete the gradient, BHK cells were transfected with MCHR1 without the VSVg tag, and a basic pH detergent-free sucrose gradient isolation was performed. The twelve fractions obtained after centrifugation were run on a 10% SDS-PAGE gel to blot for receptor and a 12% SDS-PAGE gel to blot for caveolin-1.

Caveolin distribution is at the highest density in fractions 4, 5 and 6 at a molecular weight of approximately 24 kDa (Figure 9A). MCHR1 distribution is from fraction 4 to the bottom of the gradient, but there is a density increase seen in fractions 5 and 6. As with the blots seen for the different lysing solutions (Figure 7A&B), there are multiple bands of MCHR1 present in each fraction. The lowest molecular weight marker is present in only fractions 5 and 6, and corresponds to a molecular weight of approximately 44 kDa. In the rest

Isolation of Lipid Rafts using Untagged MCHR1

A.

B.
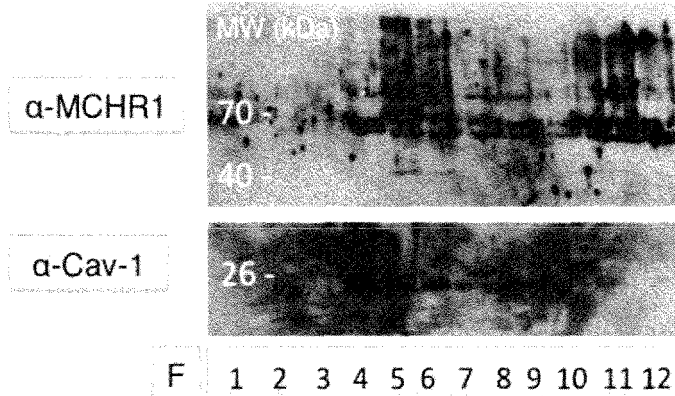
Bradford Analysis of MCHR1
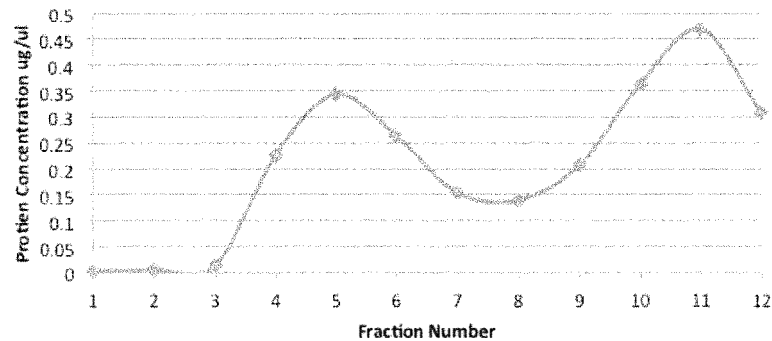
Figure 9: BHK-570 cells transfected with untagged MCHR1 (Missouri S&T cDNA Resource Center) and lipid rafts were isolated using the basic pH isolation technique and separated on a sucrose gradient.

A. The MCHR1 gel was loaded with 20 µL of sample and blotted using a 1:500 concentration of rabbit anti MCHR1 antibody, and the Caveolin-1 gel was loaded with 5 µL and blotted using a 1:2000 concentration of rabbit anti Caveolin-1 antibody.

B. Bradford analysis of fractions collected from the isolation.

of the fractions, there are bands corresponding to a molecular weight of approximately 50 kDa, with higher weight smears above all the fractions.

Bradford analysis shows that there is little protein at the top of the gradient, and fractions 4-6 contain 33% of the total protein (Figure 9B). There is a decrease in protein for fractions 6 and 7, then the largest amount of protein from fractions 9-12—a total of 49% for those fractions.

Determination of internalization of MCHR1

Initially, work was performed to determine the end location of receptor internalization. This was studied by staining BHK cells for the receptor and one of the Rab proteins. Two Rab proteins were studied, Rab5 and Rab7, Rab5 is known to associate with early endonucleases and Rab7 with late endonucleases (Stenmark et al., 1995; Bucci et al., 2000). These experiments were not successful, however, due to poor staining of the receptor. Very few changes in distribution were seen in response to treatment, even with the inefficient staining. This indicated that the internalization of the receptor needed to be studied more directly.

To determine if internalization could be visualized, overall expression of receptor was studied in a BHK model system over varying hormonal treatments. To do this, cells were transfected with VSVg-tagged MCHR1 and then plated onto cover slips; the VSVg tag was used due to the higher quality

antibody for VSVg over that of MCHR1. The transfected BHK cells were treated with 1µM MCH in DMEM- for either 0, 30 or 60 minutes. The control group of no treatment (0 time point) was given DMEM- for 60 minutes. They were then fixed and stained using fluorescent antibodies to mark VSVg-MCHR1. Cells were observed (Figure 10) to have a widespread distribution of VSVg, with slightly higher localization near the nucleus. The distribution visualized does not clarify whether the receptor is within the cytosol or on the membrane. There was visually little difference in receptor distribution between the various treatment times, and no distinct internalization of the receptor from the membrane. There is no concrete internalization seen, unlike systems that have co-transfection with arrestins. This low internalization is substantiated by the internalization seen in the ELISA data performed by our lab, and showed that there was internalization of receptor of 15 percent (Moden, 2012).

Effect of treatment with MCH on localization of MCHR1 to Caveolae

As previously described (Figure 10), there does not seem to be internalization of receptor due to MCH treatment. In addition, co-localization between MCHR1 and caveolin-1 has been verified using multiple isolation methods. It is possible that the interaction between the receptor and caveolin-1 is the cause of receptor desensitization. To determine if there is a change in receptor localization on the membrane due to hormone treatment, BHK cells

Effect of MCH Treatment on Distribution of MCHR1
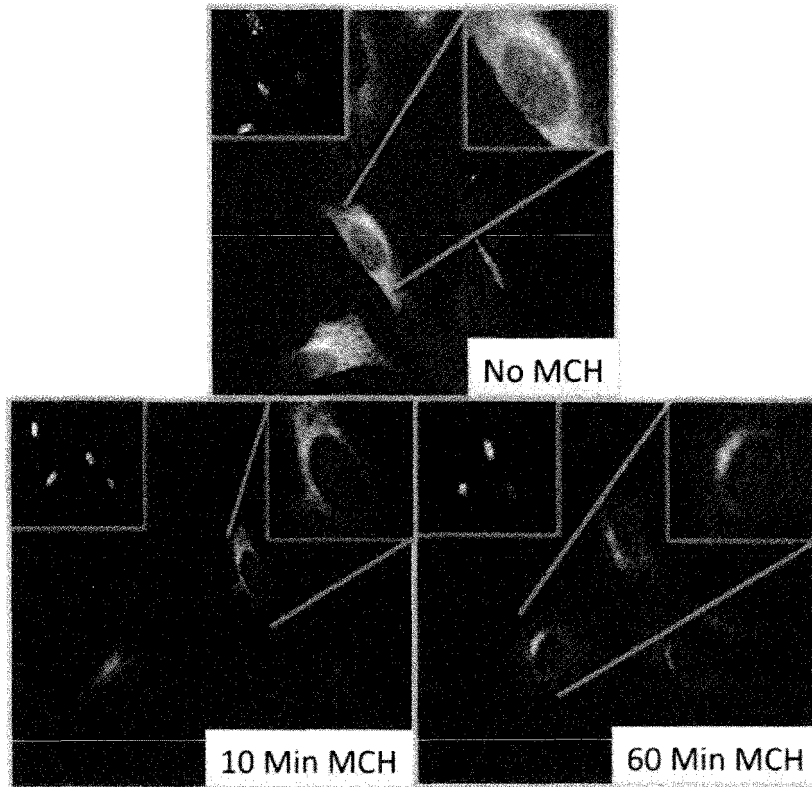
Figure 10: BHK-570 cells were treated with 1 µM Melanin-Concentrating Hormone for 10 or 60 minutes. Cells were transfected with VSVg-MCHR1 using the plasmid provided by G. Milligan, and stained using rabbit anti VSVg at 1:1000 concentration. The upper left box is an image of DAPI staining at 1:500 concentrations displaying the nucleus. The control treatment of no MCH received DMEM- for the same time the treated cells did. One cell is enlarged in each image to show the distribution of MCHR1 over the whole cell.

were transfected with VSVg-MCHR1. One set was treated for thirty minutes

with 100nM Melanin-Concentrating Hormone in serum free media, and the

other was given serum free media as a control. The cells were lysed using the

detergent-free basic pH isolation method, in collaboration with

Laurie B. Cook. The isolated fractions were run using a 10% SDS-PAGE gel

for the VSVg-MCHR1 blot and a 12% SDS-PAGE gel for the caveolin-1 blot.

Both blots were treated with the VSVg antibody and the caveolin-1 antibody

correspondingly.

For the caveolin-1 blots, there were distinct bands seen in fractions 4

and 5 in each blot (Figure 11A). Trial run 1 shows more caveolin-1 in the

lower fractions, but this can be attributed to the pipetting during production of

that sucrose gradient. For the VSVg blots, there is a greater density seen in

fractions 4 and 5 (Figure 11A), with the multiple higher molecular weight

bands seen in previous blots (Figure 7A and Figure 11A). For each of the

gradients, there is a distribution of VSVg across the bottom of the gradient.

This could be receptor being produced or those in transport to the membrane,

but it does not seem to be highly associated with caveolin-1.

There seems to be a MW shift in the upper band of the VSVg-MCHR1

blot that corresponds with the treatment of hormone, as depicted in the

turquoise boxes (Figure 11A). There appears to be a change in the

distribution of the receptor smear above 50kDa in weight. These blots suggest

that some of the receptor is disappearing from this high molecular weight.

51

MCHR1 Localization After Treatment with MCH

A.

	No MCH	30 Min MCH	
α-VSVg			Trial 1
α-Cav-1			
α-VSVg			Trial 2
α-Cav-1			

F 1 2 3 4 5 6 7 8 9 10 11 12   1 2 3 4 5 6 7 8 9 10 11 12

B. Bradford Analysis

- Trial 1 No MCH
- Trial 1 30' MCH
- Trial 2 No MCH
- Trial 2 30' MCH
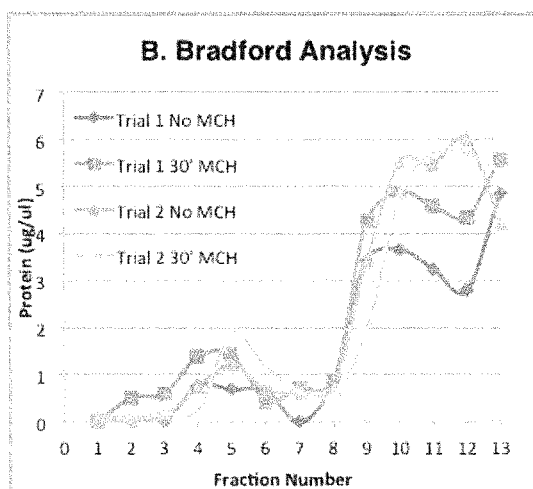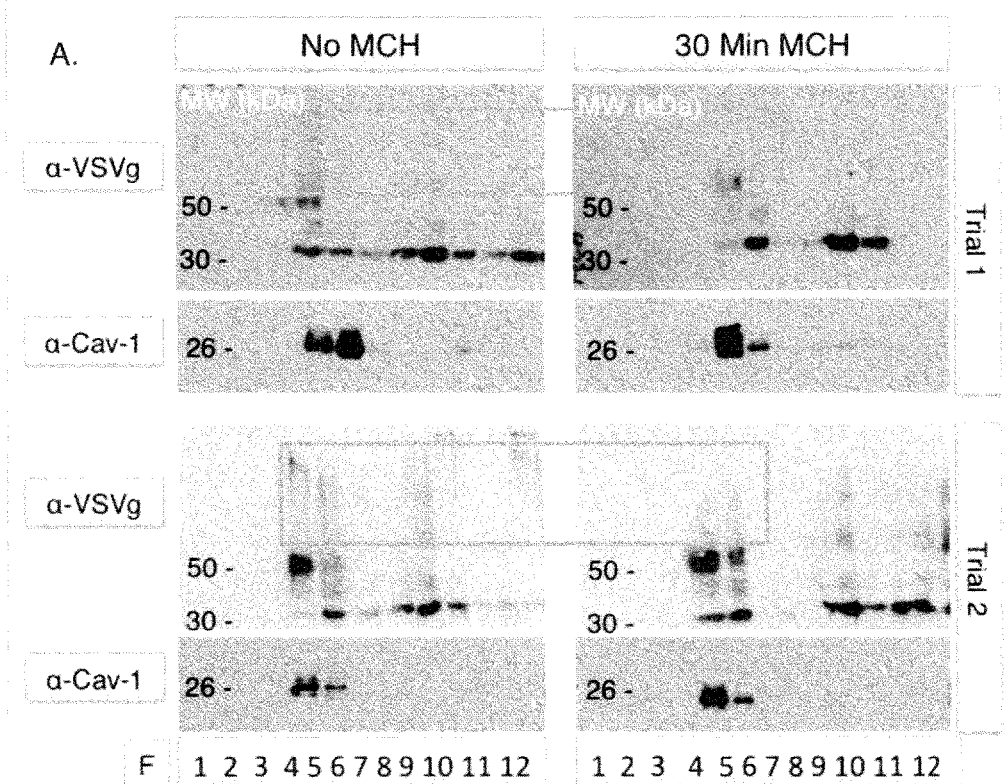
Figure 11: BHK-570 cells were transfected with VSVg-MCHR1 (G. Milligan), isolated using the basic pH method and western blots were performed. **A)** The VSVg-MCHR1 gels were blotted using a 1:2000 concentration of rabbit anti VSVg antibody. The Caveolin-1 gels were blotted using a 1:2000 concentration of rabbit anti Caveolin-1 antibody. The trials were run in collaboration with Dr. Laurie Cook. **B)** Bradford analysis of the four isolations run, trials 1 and 2 were averaged.

This could be caused by a change in the receptor, either a dimerization loss or a modification due to phosphorylation or ubiquitination.

Bradford analysis shows that there is little protein in the top of the gradients, with concentration increasing at fractions 4 and 5, decreasing through fractions 6 to 8 and then increasing again to the highest levels at the bottom of the gradient, as is normal for a lipid raft isolation (Figure 11B). In response to treatment of MCH, there is no visible change in localization of receptor within lipid rafts. This means that it is not the transition of receptor in to or out of lipid rafts that is causing the desensitization, as it is not occurring. Desensitization could occur though one of the other methods previously mentioned, such as receptor modification, which is suggested by the MW shift seen in these blots. What exactly is happening is unclear, however, and more work must be done.

Effect of β-Arrestin co-expression on localization of MCHR1

To further examine the dynamics of MCHR1 and caveolin-1 interaction, the effect of arrestin expression was studied. Work performed by our lab shows that there is a decrease in the surface expression of receptor if β-Arrestin 1 is present, and that both of the arrestins cause a greater increase in the internalization of MCHR1 (Moden, 2012). It was theorized that if the addition of the arrestins caused internalization, they might affect the interaction of caveolin-1 and MCHR1.

In order to determine the effects the arrestins had on gradient location of MCHR1, BHK cells were transfected with VSVg-MCHR1 and either pCDNA3 (as a control for the arrestin plasmids), β-Arrestin 1 or β-Arrestin 2. The cells were treated with either 100nM MCH in serum free media, or serum free media as a control, and then the cells were lysed using the basic pH detergent-free method. Initially, the collected fractions were pooled to reduce the number of western blots that had to be performed. This pooling was performed by combining fractions 1 to 3, fractions 4 to 6, fractions 7 to 9 and finally fractions 10 to 12. Western blots were performed for caveolin 1 and VSVg-MCHR1 as previously described. To look at the specific changes between the treated and untreated gradients, untreated and treated pooled fractions were run side-by-side. There is no protein in the top pooled fraction, and very little in the bottom two pooled fractions, so these were omitted.

In the pooled fraction containing fractions 4-6, there is an increase in the amount of caveolin-1 and in the VSVg-MCHR1 (Figure 12). There is much more receptor displayed in the pCDNA3 isolations, with less for each of the β-Arrestins. Each of the VSVg blots show the three distinct weight bands as described previously. What is clearer here, however, is the change in the density of the upper weight of the VSVg-MCHR1 (Figure 13). There is less protein in the upper band after treatment, which is approximately at 80 kDa. There is also a shift up of about 10 kDa from untreated to treated cells (depicted by the turquoise lines), possibly signifying a modification of

β-Arrestin Effect on MCHR1 Localization to Caveolae
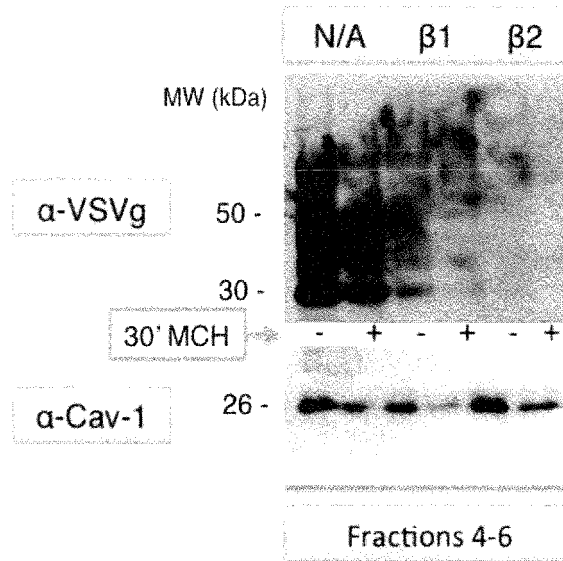
Figure 12: BHK-570 cells were transfected with a combination of VSVg-tagged MCHR1 and either pCDNA3 (negative control), β-arrestin 1 or β-arrestin 2 (J. Benovic). These cells were then treated for 30 minutes with 100nm MCH or with just DMEM- as a control. After treatment the cells were lysed using the pH 11 protocol and sucrose gradients were produced. Initially, pools were made of the fractions, so that fractions 1-3 became the first pool, then 4-6 the second and so on so that there were 4 pooled samples for each fraction, above shows fractions 4-6. Western blots were performed so that untreated and treated pools were side by side with pCDNA3, β1 and β2 in that order. The VSVg-MCHR1 gels were blotted using a 1:2000 concentration of rabbit anti VSVg antibody, while the Caveolin-1 gels were blotted with a 1:2000 concentration of rabbit anti Caveolin-1 antibody.

55

Modification of MCHR1 due to MCH treatment
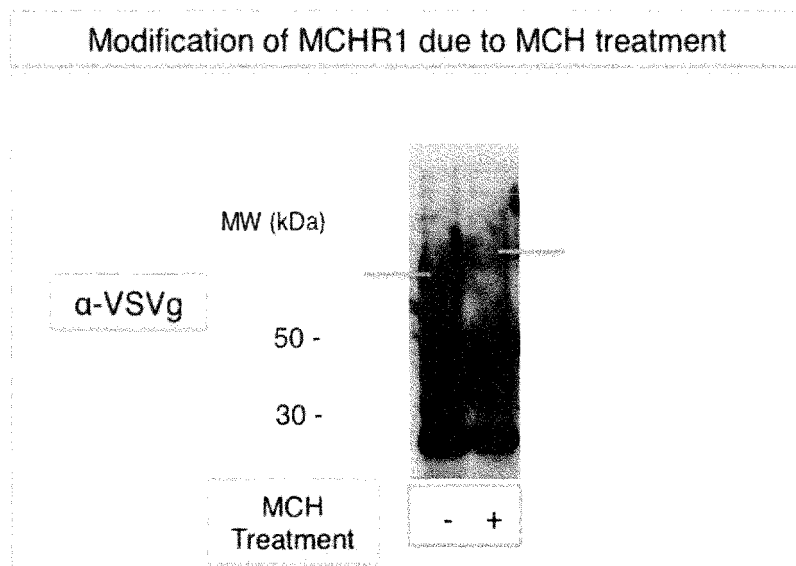
Figure 13: Further analysis of the VSVg-MCHR1 western blot performed with the β-Arrestin experiment (Figure 12). There is a change in the weight of the largest weight band as is seen by the marked lines.
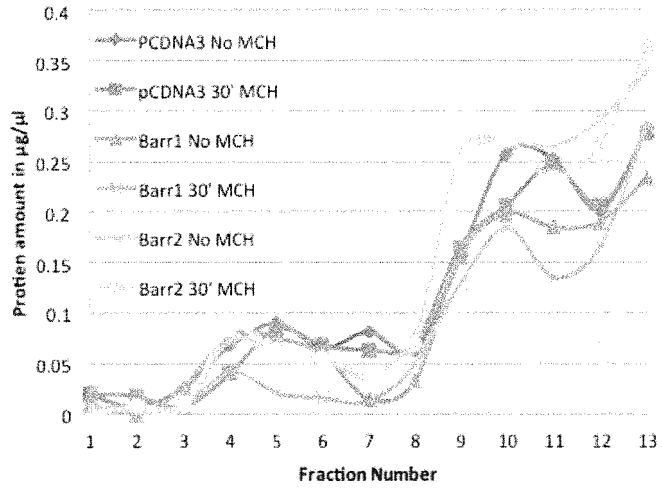
Figure 14: Bradford analysis of β-arrestin experiment (Figure 12). Full gradients from each transfection were analyzed for protein content in μg/μl.

MCHR1—possibly a phosphorylation of the receptor. Bradford analysis shows that there is the same amount of protein in each of the gradients and that each gradient follows the normal isolation amounts for isolation of caveolae at fractions 4 and 5 (Figure 14).

Discussion

Hormonal regulation of metabolism and satiety is a complex system that has many inputs and feedback system. Understanding each step of this path is very important, as it can provide possibilities for hormonal treatment of obesity. One of these hormones is melanin-concentrating hormone. Most of the current literature on MCH focuses on its effects in the brain, and few studies are performed in peripheral tissues. This thesis focuses on MCH and its receptor MCHR1 and the dynamic regulation of receptor function and desensitization.

Lipid raft isolation using CHO cells

Lipid raft domains are known to be detergent insoluble due to high levels of cholesterol, GPI-anchored proteins and glycosphingolipids (Hooper, 1999). The presence of these lighter weight lipids causes the lipid raft sections of the membrane to be isolated from the rest of the membrane via a sucrose density gradient (Smart, 1995). Various lysing methods can be used to isolate caveolae from the membrane, and each varies in the solution used to lyse the cells (Liu, 1998). Song *et al.* showed that a sodium carbonate lysate void of detergents was effective at isolating Ras, c-Src, $G_{i2\alpha}$ and $G_{\beta\gamma}$ co-localize with caveolae (Song, 1996). Prior work performed by our lab showed that MCHR1 was localized within caveolae while clathrin was at the bottom of the gradient (Cook, 2008).

In order to determine whether the detergent-free isolation could again be performed successfully, stable CHO-K1 cells were lysed and lipid rafts were isolated. As seen from the blots (Figure 3), there is normal distribution of caveolin-1 and a corresponding distribution for VSVg-MCHR-1, with enrichment occurring in fractions 4 and 5, as was published by our lab and also observed by Song *et al.* in their aforementioned work (Song et al., 1996). Bradford analysis shows that there is a small increase in the amount of protein in these fractions, but that the majority of the protein in the gradient is at the bottom. This implies that the floating of the lipid rafts is not due simply to a large amount of protein at fractions 4 and 5, but in fact due to successful isolation of the lipid raft domains from the rest of the cellular debris.

Isolation of lipid rafts using alternative lysing methods

As mentioned previously, isolation of lipid rafts can be performed in a few different ways. The original method used was the detergent-free basic pH isolation as reported by Cook and Song (Song, 1996; Cook, 2008). It is conceivable, however, that isolation of the receptor to the lipid rafts was caused by the lysing method due to molecular changes caused by the lysing solution (Anderson, 1998).The insulin receptor is co-localized with caveolae when isolated with the basic pH method, but that localization is lost when the isolation is performed with detergents (Gustavsson et al., 1999). It is theorized that the method of membrane perforation could cause molecules to

unintentionally cluster with the impermeable lipid rafts, causing unnatural co-localization (Mayor and Maxfield, 1995). Triton X-100 addition to free-floating lipids causes them to aggregate and form micelles, suggesting that the addition of the detergent to the membrane may cause aggregation of lipids (Heerklotz, 2002). As there are pros and cons to each isolation method, more than one must be examined to determine the extent of co-localization.

The two other methods used were a detergent isolation using Triton X-100 and a different detergent-free isolation using an osmotic gradient created with sucrose for lysis, both previously reported by Liu *et al.* and Smart *et al.* (Smart , 1995; Liu , 1998). The Triton X-100 isolation was performed in a cold room and on ice to get the coldest temperature possible, as this helps to maintain the stability of the lipid rafts. Triton X-100 isolates lipid rafts best when at a 4° C temperature, while at 37° C the isolation becomes imperfect (Brown and Rose, 1992). As can be seen from the gradients, the distribution of caveolin-1 along the gradient is much greater in both methods of isolation then seen in the CHO cell isolation (Figure 4). There are a few reasons for this, for the Triton X-100 isolation, it is imaginable that the gradients and cells were not kept cold enough. If the cells were not kept at the optimum $4^{o}C$, the stability of the lipid rafts would have been compromised. In the case of the osmotic isolation, there was already sucrose in the lysing solution. This could have caused a change in the densities of the gradient, and changed the distribution of the caveolin-1. Also, the lysing procedure could have been less

effective as the only method of isolation was through a slight osmotic gradient and pulverization. Despite the inefficient isolation of caveolae, it appears that there is a correlation between the amount of caveolin-1 and VSVg-MCHR-1.

Isolating caveolae via Triton X-100 is more delicate than other methods, and the molecules that are maintained within the domains via this method can vary and can depend on the amount and type of detergent present (Pike, 2003). It is possible that for the detergent isolation, too much detergent was used, which compromised the isolation abilities. Isolations done isolating Ras with caveolin-1 showed high amounts of Ras and cav-1 at fractions 4/5 with a slight amount of protein from fraction 8 to the bottom of the gradient (Kawabe et al., 2001). Also, isolations performed on matrix-metaloproteases (MMP's) showed similar distribution of both the MMP's and caveolin-1, with slightly more of each at the bottom of the gradient (B et al., 2001). These are comparable to the originally performed CHO-K1 isolations (Figure 3), and to the previously published work performed using the basic pH solutions (Cook et al., 2008). The gradients performed here, however, show greater distribution of both caveolin-1 and receptor across the bottom of the gradient (Figure 4), and the isolation methods were not as exact as hoped.

The isolations show that there is a correlation between the density and localization of caveolin-1 and VSVg-MCHR-1. The detergent-free basic pH isolation method previously published seems to be the best at maintaining the caveolae structure for proper isolation (Cook et al., 2008). The correlation

between receptor amount and caveolin is maintained for each isolation method, but the type of lipid rafts isolated through the basic isolation method are the most defined.

Verification of distribution of untagged MCHR-1

It is conceivable that adding the VSVg tag to MCHR1 causes a change in the localization of the receptor on the membrane. To further investigate this potentiality, a western blot was performed for MCHR1 without the VSVg tag. Epitope tagging was performed by genetically inserting a well-characterized antigen into a plasmid of the desired protein. During transfection, the tag was added onto the desired molecule (in this case MCHR1) and provided an easy way to target for the molecule. While the VSVg tag is small—11 amino acids in size—it could interact with surrounding molecules on the membrane surface. Epitope tags have been used previously due to the higher quality of the antibody for the VSVg molecule in comparison to the MCHR-1 antibody. If the blots for VSVg and MCHR1 are compared (Figure 11 and Figure 9), it can be seen that the background of the MCHR1 blot is dirtier. Numerous attempts were run of the MCHR1 blot, and the one reported showed the best antibody blotting. The correlation seen in these blots show that there is co-localization between MCHR-1 and caveolin-1. This interaction is present regardless of the type of isolation, or the tag that is placed on the receptor.

Determination of internalization rate of MCHR1

In order to determine the internalization of MCHR1 after agonist treatment, fluorescent microscopy was performed. After analysis of the distribution of MCHR1 over the cell surface at given treatment times, very little internalization is seen (Figure 10). There is uniform distribution across the entirety of the membrane and the cytosol, with slightly higher concentration around the nucleus, possibly in the ER or Golgi. This distribution has also been seen for other receptors such as insulin in adipose and P2X receptors in neurons (Khakh, 2001; Hunker, 2006). After treatment, however, there is little difference in the distribution of the receptor. The same patterns are seen after 10 and even 60 minutes of 1μM MCH treatment. This treatment amount was used to ensure that complete saturation of the receptor was achieved. The K_d of MCHR1 is 3.1 ± 0.4 nM, and this experiment was performed in an overexpression model, so by treating with 1μM MCH complete saturation was ensured (An, 2001).

This lack of internalization is in contrast to work performed by Saito *et al.* who determined that there was internalization of 21.9% seen in as little as five minutes, and a greater internalization rate of 44.2% seen after 30 minutes of treatment (Saito, 2004). Past work performed by Katrina Haude, an undergraduate in our lab, shows that if either β-Arrestin is included in transfection, there is an internalization of receptor from the membrane (Figure

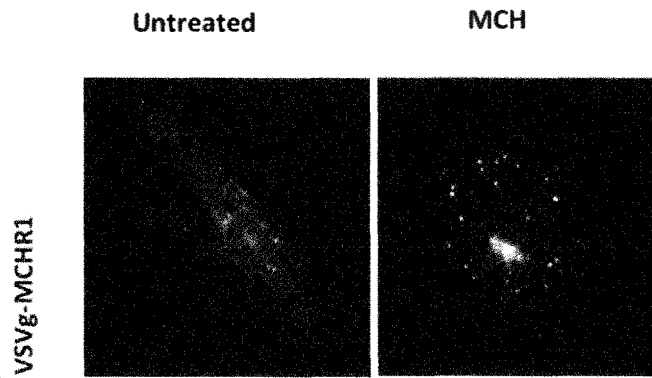## Effect of β-Arrestin Expression on Internalization of MCHR1

Image by Katrina Haude

Figure 15: Transfected BHK cells with β-Arrestin 1 and Vsvg-MCHR1. Images are of receptor distribution before and after MCH treatment.

15) (Moden, 2012). By comparing this marked internalization with the results provided of MCHR1 internalization (Figure 10), it can be seen that if there are no additional parts of the clathrin pathway added, internalization does not visibly occur. This does not mean that there is not internalization, however, as there could be very low internalization that cannot be visualized. Using fluorescent microscopy in this way would not show other changes occurring on the membrane. As this is a transfected receptor model, there could be an overwhelming amount of receptor on the membrane, and so the sheer number of receptors present would cause the movement of receptors on the membrane or interactions between receptors to change.

Effect of treatment with MCH on localization of MCHR-1 to caveolae

If desensitization is caused by interactions with caveolae, the effect of treatment with MCH on localization within lipid rafts must be examined. After analysis of the gradients, there is little change in the overall location of receptor within caveolae (Figure 11). This is not unusual. There are examples like the EGF and PGDF receptors that are associated with caveolae without agonist, but after agonist addition are only transiently associated (Matveev and Smart, 2002). Another example is the angiotensin II type 1A receptor (a $G_{\alpha q}$ GPCR) which is associated with caveolae regardless of agonist addition (Ishizaka et al., 1998). This lack of change in the localization of receptor within lipid rafts may mean that internalization is not the reason that there is

desensitization occurring with MCHR1, possibly supported by the results of the fluorescent images reported earlier (Figure 10).

There have been reports of internalization of caveolae to either endosomes or to an internal structure known as a caveosome. Work done looking as low-density lipoproteins undergoing transcytosis across endothelial cells showed that the LDL's crossed through the caveosome structures through caveolae endocytosis (Candela et al., 2008). So if there is the same level of LDL's in the caveosome as in the membrane caveolae, the caveosome should be approximately the same weight as membrane domains.

If there was internalization to a caveosome, there is the potential that the small amount of receptor internalized could not be visualized in the fluorescent images (Figure 10). While caveosomes are large structures, there would have to be a large quantity of internalized receptors to visualize the caveosome. Preliminary work done by our lab using confocal and electron microscopy performed on differentiated 3T3L1 cells showed large vesicular bodies that could have been large membrane caveolae or even internalized caveolae. It is imaginable that there are internal caveosomes shuttling caveolae and receptors to and from the membrane, and that the activated receptor is removed from the membrane via this pathway, but that it could not be visualized due to the low amount of internalization. It is also likely that there is a conformational change occurring of the receptor within the lipid rafts.

This change could be switching off the activity of the receptor while maintaining the overall concentrations within caveolae.

Effect of β-Arrestin co-expression on localization of MCHR-1

Work done previously by Katrina Haude shows that there is visual internalization due to MCH treatment when one of the β-Arrestins is incorporated into the cellular model (Figure 14) (Moden, 2012). So the effect that transfection with either β-Arrestin1 or β-Arrestin2 has on the co-localization of receptor to lipid rafts was studied. As was seen in the western blots, there is a decrease of the receptor seen when an arrestin is incorporated (Figure 12). This is interesting, as there is still normal expression with the pCDNA3 transfection, and as the Bradford analysis of each set of fractions is essentially the same.

So there is some sort of hindrance occurring when the arrestins are present in the packaging of receptor within the lipid rafts, or there is a change in the activity of the receptor with arrestins, requiring less receptor to be present. When comparing this information with work performed by Jay Moden using ELISA analysis of surface expression of receptor, there are some correlations. When the cells were transfected with β-Arrestin 1, there was less receptor visualized on the external surface of the receptor. This corresponds to the decreased expression seen on the β-Arrestin 1 gradient, and so there may be some hindrance occurring due to the arrestin recruitment, less

transfection of the receptor itself or even more degradation of the receptor due to the presence of the arrestin. In the instance of cell surface expression for β-Arrestin 2, there was approximately the same amount of receptor seen as for the pCDNA3 model. This could signal a better relationship between MCHR-1 and β-Arrestin 2, a theory that has been studied previously by Evans *et al.* They reported that in cells were triple-transfected with tagged-MCHR1, GRK2 and either β-arrestin 1 or 2. In the cells expressing β-arrestin 2, there was selective recruitment to the plasma membrane. This association with receptor was transient, and internalization of both β-Arrestin 2 and the receptor in conjunction did not occur (Evans et al., 2001). It is important to note that their work was performed with GRK, and experiments done by our lab did not have this triple-transfection protocol, and transfection with either β-Arrestin showed internalization. When neither of the arrestins are present, however, there is increased expression seen throughout the gradient and co-localization with caveolae is more pronounced.

Internalization of upper weight MCHR1 due to MCH treatment

While analyzing the western blots comparing treated cells with untreated cells, a pattern emerged. Before treatment, the VSVg-MCHR-1 western blots showed a band with a molecular weight at around 40 kDa, and this would be the receptor without any modification or dimerization. The known molecular weight for MCHR1 is at 46 kDa, which is the largest density

69

band seen on the western blots, concurring with the normal size of the protein (Bittencourt et al., 1992). The slight difference in size could be due to the gel run, with possible variations in the segregation. Above this weight is a smear that goes to the top of the gradient, which could be composed of dimers or even oligomers of MCHR1. Work performed using Fluorescence Resonance Energy Transfer (FRET) of fluorescently tagged luteinizing hormone has shown that on the cellular surface, FRET has been detected between multiple hormone bound luteinizing hormone receptors. This suggests that the LH receptor is a functional dimer on the cellular surface. Interestingly, FRET was dependent on the receptor's signaling potential, with no FRET seen with mutant receptors, signifying that active receptors need to interact to be functional (Roess, 2000). Within the Tumor-Necrosis Factor-α family, it is believed that agonist-promoted dimerization forms an equilibrium, which is thought to be an important step in receptor activation and deactivation (Weiss and Schlessinger, 1998; Schlessinger, 2000). If this activation/inactivation equilibrium is true for MCHR1, than the loss of the upper weight dimer after treatment would mean that the active form of the receptor is a dimer or even an oligomer, as the highest weight band is more then double the 46 kDa weight of the single receptor.

Mode of Receptor Desensitization Theory

For a receptor to be desensitized, there must be a lack of active receptor on the membrane. As mentioned previously, there are different ways that cells accomplish this task. This thesis considers two possible methods of desensitization. First, the receptor could be modified to become unresponsive to hormone treatment. Second, the receptor could be removed from the membrane through an endocytosis method. Work done by our lab showed that MCH treatment causes an increase in activated ERK, and that after a second treatment thirty minutes later there was not the same rate of activation (Figure 16). Initially, it was thought that internalization of the receptor via the clathrin pathway was the cause for this long period of desensitization, as proposed by Saito *et al.* (Saito , 2004). Work shown by fluorescent imaging in this report and ELISA data reported by Jay Moden (Figure 17), however, showed that without transfection with parts of the clathrin pathway, there is not a large percentage of internalization seen in response to MCH treatment.

This means that there could be an alternative way in which the cell is desensitizing to hormonal stimulation. The proposed alternative is through co-localization and interaction with caveolae. This interaction was present despite the method of isolation or the tag associated with the receptor. If part of the arrestin pathway is added, then a greater internalization is seen, but in the case of β-Arrestin 1 there is less receptor seen on the surface. Additionally, studies performed looking at co-localization before and after

71
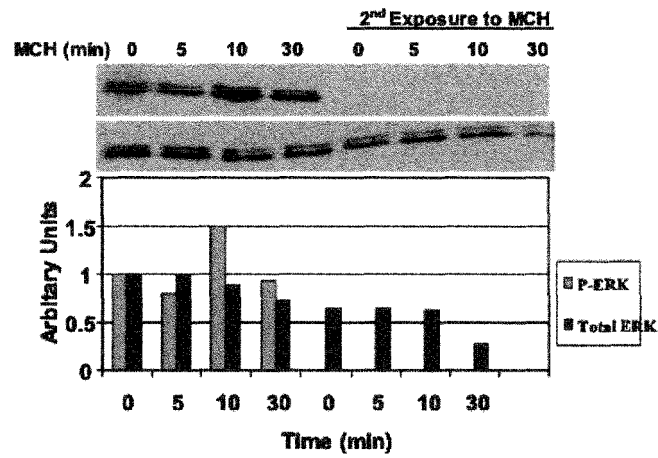
Figure 16: Desensitization of MAPK activation following an initial MCH exposure. MAPK activation was measured using antibodies to total and phospho-ERK. Work performed by Makoto

Comparison of MCHR1 Surface Expression with Arrestin ± 30 Minutes of Agonist Exposure
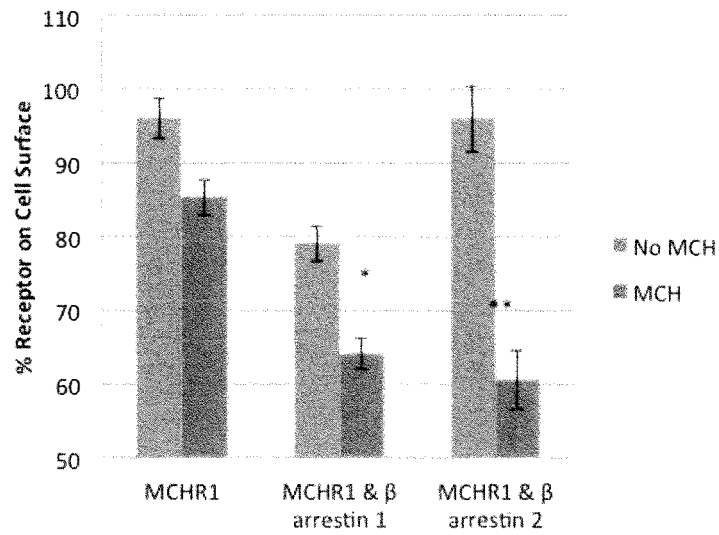
Figure 17: BHK570 cells were transfected labeled with anti-VSVg in a modified cell surface-ELISA. Chart shows the loss of surface immunoreactivity after 30 min MCH for cells expressing receptor alone or receptor with either B-arr1 or B-arr2 are compared. *indicate statistical significance (Moden, 2012)

hormone treatment showed that there is a loss of an upper-weight band of the receptor, and a possible phosphorylation event is occurring (Figure 13). No other lab has published work showing a phosphorylated form of MCHR1, so this could be an exciting development. It could relate to the work showing inactivation of the receptor if certain amino acids are deleted, as discussed previously (Tetsuka et al., 2004). If these are taken in conjunction, it can be theorized that MCHR1 is localized to caveolae and that some interaction occurring within caveolae is causing desensitization.

Caveolin-1 can interact with receptors within caveolae by complexing with the molecule, and then dissociate when the receptor is activated. If this is the case for MCHR1, then the reactive form of the receptor could be dissociating from caveolae after activation. This interaction was published by our lab through immunoprecipitation experiments showing that caveolin-1 and MCHR1 immunoprecipitate in conjunction with one another (Cook et al., 2008). If this is taken in combination with the ELISA data showing that there is roughly 15% internalization, then it can be theorized that the dissociated receptor is internalizing. If parts of the arrestins are included in this theory, then the association between the arrestins and the receptor could be more readily pulling the active receptor out of caveolae and internalizing it. This idea was discussed previously in relation to the insulin receptor and its movement into and out of caveolae, with signaling only occurring when the

receptor is within caveolae (Gustavsson et al., 1999). A similar process could be occurring with MCHR1 and movement with caveolae.

Interestingly, work performed by Robert Carroll working with an RNAi for caveolin-1 and looking at leptin production in response to MCH stimulation, showed that if caveolin-1 is depleted, then there is a greater production of leptin. Combining this with the theory that dimers or oligomers of the receptor are the active form of the receptor, then it is conceivable that the receptor interaction with caveolin-1 is causing less of the active dimer to be available. If caveolin-1 is removed, then this hindrance disappears, and there are more dimers formed and more leptin produced in response to MCH treatment.

How could this all add up to desensitization? In summary, co-localization with caveolae could cause there to be fewer of the dimerized receptor available on the membrane. After activation, these dimerized receptors may dissociate from caveolin-1 and be removed from the membrane, or dissociate from one another, becoming inactive in response to MCH treatment. The interaction between caveolin-1 and MCHR1 could potentially inhibit the formation of new dimers, and so possibly contribute to the time required to re-sensitize. This could explain why signaling occurs at a larger rate without caveolin-1.

Future Directions

To further verify the proposed method of desensitization, there are a few key experiments that could be performed. Caveolin-1 does interact with MCHR1, so it should be determined whether dimers of MCHR1 form and if they are the active form of the receptor. This could be done using FRET analysis, tagging MCH with various fluorescent proteins, such as Cyan-fluorescent protein and Yellow-fluorescent protein, and determining if there is FRET seen between two receptors on the membrane, as previously described in the Luteinizing Hormone example (Roess et al., 2000). The FRET analysis could be taken further, to determine if FRET is dependent on the signaling potential of the receptor, and potentially proving that the dimer is the form of the receptor that is activated. If possible, the kinetics of dimer association and disassociation could be determined both within caveolae and in an RNAi caveolin-1 deficient model. This could help determine why the signaling potential of MCHR1 is greater without cholesterol than with cholesterol.

Finally, more work should be done with an even more physiologically relevant model, like the 3T3-L1 adipose cells. Additional work should be done to visualize MCHR1 in adipocytes using fluorescent microscopy, and continuing on into confocal microscopy. Very preliminary work performed (not reported due to time constraints) on the confocal microscope showed that there was co-localization visualized between caveolin-1 and MCHR1. This work should be continued to better verify the co-localization and determine

76

the effects of MCH treatment in the physiologically relevant 3T3 model. If a better isolation method could be determined, then further work with lipid isolations could be performed. In attempts to perform a sucrose gradient with 3T3-L1 differentiated adipocytes, there was beautiful distribution of caveolin-1 seen, but there was too little MCHR1 to successfully blot for the receptor.

Finally, more studies should be done on the changes seen in the receptor weight before and after MCH treatment. This was performed only three times, and more data should be collected to verify that there is a change in the upper weight densities on the western blots.

Significance

Treatment of obesity has become a very important goal of drug companies. Initial work with MCHR-1 inhibitors has shown much promise in animal models, but there is potential for problems to occur in human trials. In this way, it is very important to understand the complete satiety pathway to identify possible complications. Understanding the purpose of MCHR1 in adipose cells and the signaling properties of the receptor may help in understanding the overall effects of inhibitors on the human body. As obesity is a growing epidemic, there is a greater need for a weight-loss booster. In the cases of individuals who eat healthily and exercise regularly and yet still cannot lose weight, understanding the hormonal pathway could spur a new method of treatment to correct their imbalance and help them succeed. To be

successful in the treatment of obesity, the entire satiety pathway, including

MCH and its effect on peripheral tissues, must be examined.

Appendix 1

Solution Recipes

10X Phosphate Buffered Saline
　　　　To 800 mls of dH_2O, add:
　　　　　　　80g NaCl
　　　　　　　2g KCl
　　　　　　　14.4 g Na_2HPO_4
　　　　　　　2.4 g KH_2PO_4
　　　　pH to 7.4 and bring up to 1 L
PBS- T
　　　　To 1 Liter of 1X PBS, add 1 mL of Tween-20
5X Bradford Reagent
　　　　1)　Dissolve 100mg Coomasie Blue in 50mL of EtOH
　　　　2)　Add 100mL 85% Phosphoric acid
　　　　3)　Add 50mL dH_2O
　　　　4)　Filter into clean container

Mes-Buffered Saline

　　　　25mM Mes (Acros Organics)
　　　　0.15 M NaCl
　　　　pH to 6.5

MBS with 250mM Na_2CO_3

　　　　To 400 mL MBS add:
　　　　13.25g Na_2CO_3
　　　　pH to 11 and fill to 500 mL

500 mM Na_2CO_3 Lysis Solution

　　　　Add to 400 mL dH_2O:
　　　　26.6 g Na_2CO_3
　　　　pH to 11 and fill to 500 mL

Triton Lysis Solution

　　　　To 500 mL of MBS add 0.5 mL of Triton X-100

Neutral Lysis Solution

    25mM Tris
    250mM Sucrose

5X Lamelli Sample Buffer

    3.75mL, 1.0M Tris HCL, pH 6.8
    1.5g SDS
    0.075g Bromophenol Blue
    1.16g Dithiothreitol (Cleland's Reagent)
    Bring up to 7.5 mL dH_2O. Add 7.5 mL glycerol.

10X SDS Running Buffer

    30.3g Tris Base
    144g Glycine
    10g SDS
    Bring up to 1 Liter in dH_2O

Towbins Transfer Buffer

    To 1 Liter of water, add:
    11.6 g glycine
    23.2 g Tris Base
    1.48 g SDS
    800 ml methanol
    Bring volume to 4 Liters with water

10X Tris-Buffered Saline (TBS)

    87.66g NaCl
    12.11g Tris Base
    4mL HCL
    pH to 8.0 then bring up to 1 L with dH_2O

TBS-T

    To 1 mL of TBS add 500 μL of Tween-20

Bibliography

Alkemade, A., Friesema, E.C., Unmehopa, U.A., Fabriek, B.O., Kuiper, G.G., Leonard, J.L., Wiersinga, W.M., Swaab, D.F., Visser, T.J., and Fliers, E. (2005). Neuroanatomical Pathways for Thyroid Hormone Feedback in the Human Hypothalamus. JCEM *90*, 4322–4334.

An, S., Cutler, G., Zhao, J.J., Huang, S.G., Tian, H., Li, W., Liang, L., Rich, M., Bakleh, A., Du, J., et al. (2001). Identification and characterization of a melanin-concentrating hormone receptor. Proc. Natl. Acad. Sci. U.S.A. *98*, 7576–7581.

Anderson, R.G. (1998). The caveolae membrane system. Annu. Rev. Biochem. *67*, 199–225.

Balklava, Z., and Grant, B.D. (2006). The regulation of endocytosis by kinases: cell biology meets genomics. Genome Biology *6*, 245.

Banks, W.A., Kastin, A.J., Huang, W., Jaspan, J.B., and Maness, L.M. (1996). Leptin enters the brain by a saturable system independent of insulin. Peptides *17*, 305–311.

Bell-Anderson K.S., and Bryson J.M. (2004). Leptin as a Potential Treatment for Obesity: Progress to Date. Treatments in Endocrinology *3*, 11–18.

Berg, F.M. (1999). Health Risks Associated With Weight Loss and Obesity Treatment Programs. Journal of Social Issues *55*, 277–297.

Berthoud, H. -r. (2008). Vagal and hormonal gut–brain communication: from satiation to satisfaction. Neurogastroenterology & Motility *20*, 64–72.

Bertile, F., Oudart, H., Criscuolo, F., Maho, Y.L., and Raclot, T. (2003). Hypothalamic gene expression in long-term fasted rats: relationship with body fat. Biochem. Biophys. Res. Commun. *303*, 1106–1113.

Bittencourt, J.C., Presse, F., Arias, C., Peto, C., Vaughan, J., Nahon, J.-L., Vale, W., and Sawchenko, P.E. (1992). The melanin-concentrating hormone system of the rat brain: An immuno- and hybridization histochemical characterization. The Journal of Comparative Neurology *319*, 218–245.

Blake, C.A. (1974). Stimulation of Pituitary Prolactin and TSH Release in Lactating and Proestrous Rats. Endocrinology *94*, 503–508.

Blast (2012a). NCBI Blast:NP_005288:melanin-concentrating hormone receptor 1 compared to melanin-concentrating hormone receptor 2.

Blast (2012b). NCBI Blast:reflNP_005288.3l melanin-concentrating hormone receptor 1 rat compared to melanin-concentrating hormone receptor 1 human.

Boguski, M.S., and McCormick, F. (1993). Proteins regulating Ras and its relatives. , Published Online: 16 December 1993; l Doi:10.1038/366643a0 *366*, 643–654.

Borowsky, B., Durkin, M.M., Ogozalek, K., Marzabadi, M.R., DeLeon, J., Heurich, R., Lichtblau, H., Shaposhnik, Z., Daniewska, I., Blackburn, T.P., et al. (2002). Antidepressant, anxiolytic and anorectic effects of a melanin-concentrating hormone-1 receptor antagonist. Nature Medicine.

Brown, D.A., and Rose, J.K. (1992). Sorting of GPI-anchored proteins to glycolipid-enriched membrane subdomains during transport to the apical cell surface. Cell *68*, 533–544.

Bucci, C., Thomsen, P., Nicoziani, P., McCarthy, J., and van Deurs, B. (2000). Rab7: a key to lysosome biogenesis. Mol. Biol. Cell *11*, 467–480.

Candela, P., Gosselet, F., Miller, F., Buee-Scherrer, V., Torpier, G., Cecchelli, R., and Fenart, L. (2008). Physiological pathway for low-density lipoproteins across the blood-brain barrier: transcytosis through brain capillary endothelial cells in vitro. Endothelium *15*, 254–264.

Cantalupo, G., Alifano, P., Roberti, V., Bruni, C.B., and Bucci, C. (2001). Rab-interacting lysosomal protein (RILP): the Rab7 effector required for transport to lysosomes. EMBO J. *20*, 683–693.

Chambers, J., Ames, R.S., Bergsma, D., Muir, A., Fitzgerald, L.R., Hervieu, G., Dytko, G.M., Foley, J.J., Martin, J., Liu, W.S., et al. (1999). Melanin-concentrating hormone is the cognate ligand for the orphan G-protein-coupled receptor SLC-1. Nature *400*, 261–265.

Chen, Y. (2002). Targeted Disruption of the Melanin-Concentrating Hormone Receptor-1 Results in Hyperphagia and Resistance to Diet-Induced Obesity. Endocrinology *143*, 2469–2477.

Chini, B., and Parenti, M. (2004). G-protein coupled receptors in lipid rafts and caveolae: how, when and why do they go there? J. Mol. Endocrinol. *32*, 325–338.

Cohen, P., Zhao, C., Cai, X., Montez, J.M., Rohani, S.C., Feinstein, P., Mombaerts, P., and Friedman, J.M. (2001). Selective deletion of leptin receptor in neurons leads to obesity. Journal of Clinical Investigation *108*, 1113–1121.

Cook, L.B., Delorme-Axford, E.B., and Robinson, K. (2008). Caveolae as potential mediators of MCH-signaling pathways. Biochemical and Biophysical Research Communications *375*, 592–595.

Drel, V.R., Mashtalir, N., Ilnytska, O., Shin, J., Li, F., Lyzogubov, V.V., and Obrosova, I.G. (2006). The leptin-deficient (ob/ob) mouse: a new animal model of peripheral neuropathy of type 2 diabetes and obesity. Diabetes *55*, 3335–3343.

Fan, J.Y., Carpentier, J.L., van Obberghen, E., Grunfeld, C., Gorden, P., and Orci, L. (1983). Morphological changes of the 3T3-L1 fibroblast plasma membrane upon differentiation to the adipocyte form. J. Cell. Sci. *61*, 219–230.

Farooqi, I.S., Jebb, S.A., Langmack, G., Lawrence, E., Cheetham, C.H., Prentice, A.M., Hughes, I.A., McCamish, M.A., and O'Rahilly, S. (1999). Effects of recombinant leptin therapy in a child with congenital leptin deficiency. N. Engl. J. Med. *341*, 879–884.

Ferguson, S.S.G., Zhang, J., Barakt, L.S., and Caron, M.G. (1998). Molecular mechanisms of G protein-coupled receptor desensitization and resensitization. Life Sciences *62*, 1561–1565.

Figarella-Branger, D., Pouget, J., Bernard, R., Krahn, M., Fernandez, C., Lévy, N., and Pellissier, J.F. (2003). Limb-girdle muscular dystrophy in a 71-year-old woman with an R27Q mutation in the CAV3 gene. Neurology *61*, 562–564.

Flegal, K.M. (2012). Prevalence of Obesity and Trends in the Distribution of Body Mass Index Among US Adults, 1999-2010. JAMA: The Journal of the American Medical Association *307*, 491.

Flegal, K.M., Carroll, M.D., Ogden, C.L., and Curtin, L.R. (2010). Prevalence and trends in obesity among US adults, 1999-2008. JAMA *303*, 235–241.

Fridriksson, E.K., Shipkova, P.A., Sheets, E.D., Holowka, D., Baird, B., and McLafferty, F.W. (1999). Quantitative analysis of phospholipids in functionally important membrane domains from RBL-2H3 mast cells using tandem high-resolution mass spectrometry. Biochemistry *38*, 8056–8063.

Frishman, W.H., Cheng-Lai, A., and Newarskas, J. (2005). Current cardiovascular drugs (Philadelphia, Pa.: Current Medicine).

Fujimoto, T., Kogo, H., Nomura, R., and Une, T. (2000). Isoforms of caveolin-1 and caveolar structure. J Cell Sci *113*, 3509–3517.

Furuchi, T., and Anderson, R.G.W. (1998). Cholesterol Depletion of Caveolae Causes Hyperactivation of Extracellular Signal-related Kinase (ERK). J. Biol. Chem. *273*, 21099–21104.

Gustavsson, J., Parpal, S., Karlsson, M., Ramsing, C., Thorn, H., Borg, M., Lindroth, M., Peterson, K.H., Magnusson, K.E., and Strâlfors, P. (1999). Localization of the insulin receptor in caveolae of adipocyte plasma membrane. FASEB J. *13*, 1961–1971.

Hatcher, R.A. (1998). Contraceptive technology (New York: Ardent Media).

Hawes, B.E., Kil, E., Green, B., O'Neill, K., Fried, S., and Graziano, M.P. (2000). The melanin-concentrating hormone receptor couples to multiple G proteins to activate diverse intracellular signaling pathways. Endocrinology *141*, 4524–4532.

Heerklotz, H. (2002). Triton promotes domain formation in lipid raft mixtures. Biophys. J. *83*, 2693–2701.

Hegde, L.G., Ping, X.L., Jochnowitz, N., and Craig, D.A. (2009). The role of melanin-concentrating hormone-1 receptors in the voiding reflex in rats. J. Pharmacol. Exp. Ther. *328*, 165–173.

Hill, J., Duckworth, M., Murdock, P., Rennie, G., Sabido-David, C., Ames, R.S., Szekeres, P., Wilson, S., Bergsma, D.J., Gloger, I.S., et al. (2001). Molecular cloning and functional characterization of MCH2, a novel human MCH receptor. J. Biol. Chem. *276*, 20125–20129.

Hooper, N.M. (1999). Detergent-insoluble glycosphingolipid/cholesterol-rich membrane domains, lipid rafts and caveolae (Review). Molecular Membrane Biology *16*, 145–156.

Huang, F., Khvorova, A., Marshall, W., and Sorkin, A. (2004). Analysis of Clathrin-mediated Endocytosis of Epidermal Growth Factor Receptor by RNA Interference. J. Biol. Chem. *279*, 16657–16661.

Hunker, C.M., Kruk, I., Hall, J., Giambini, H., Veisaga, M.L., and Barbieri, M.A. (2006). Role of Rab5 in insulin receptor-mediated endocytosis and signaling. Archives of Biochemistry and Biophysics *449*, 130–142.

Igarashi, J., Thatte, H.S., Prabhakar, P., Golan, D.E., and Michel, T. (1999). Calcium-independent activation of endothelial nitric oxide synthase by ceramide. Proc. Natl. Acad. Sci. U.S.A. *96*, 12583–12588.

Ishizaka, N., Griendling, K.K., Lassègue, B., and Alexander, R.W. (1998). Angiotensin II Type 1 Receptor Relationship With Caveolae and Caveolin After Initial Agonist Stimulation. Hypertension *32*, 459–466.

Jehan, F., Neveu, I., Naveilhan, P., Brachet, P., and Wion, D. (1993). Complex interactions among second messenger pathways, steroid hormones, and protooncogenes of the Fos and Jun families converge in the regulation of the nerve growth factor gene. J. Neurochem. *60*, 1843–1853.

Kawabe, J., Grant, B.S., Yamamoto, M., Schwencke, C., Okumura, S., and Ishikawa, Y. (2001). Changes in caveolin subtype protein expression in aging rat organs. Molecular and Cellular Endocrinology *176*, 91–95.

Kawauchi, H., Kawazoe, I., Tsubokawa, M., Kishida, M., and Baker, B.I. (1983). Characterization of melanin-concentrating hormone in chum salmon pituitaries. Nature *305*, 321–323.

Khakh, B.S., Smith, W.B., Chiu, C.-S., Ju, D., Davidson, N., and Lester, H.A. (2001). Activation-dependent changes in receptor distribution and dendritic morphology in hippocampal neurons expressing P2X2-green fluorescent protein receptors. PNAS *98*, 5288–5293.

Klein, S., Coppack, S.W., Mohamed-Ali, V., and Landt, M. (1996). Adipose Tissue Leptin Production and Plasma Leptin Kinetics in Humans. Diabetes *45*, 984–987.

Labrecque, L., Royal, I., Surprenant, D.S., Patterson, C., Gingras, D., and Béliveau, R. (2003). Regulation of Vascular Endothelial Growth Factor Receptor-2 Activity by Caveolin-1 and Plasma Membrane Cholesterol. Mol. Biol. Cell *14*, 334–347.

Lebl, M., Hruby, V.J., Castrucci, A.M. de L., Visconti, M.A., and Hadley, M.E. (1988). Melanin concentrating hormone analogs: contraction of the cyclic structure. 1. Agonist activity. J. Med. Chem. *31*, 949–954.

Lefkowitz, and Freedman (1996). Desensitization of G protein-coupled receptors. Recent Progress in Hormone Research *51*, 319.

Lembo, P.M., Grazzini, E., Cao, J., Hubatsch, D.A., Pelletier, M., Hoffert, C., St-Onge, S., Pou, C., Labrecque, J., Groblewski, T., et al. (1999). The receptor for the orexigenic peptide melanin-concentrating hormone is a G-protein-coupled receptor. Nat. Cell Biol. *1*, 267–271.

Li, S., Couet, J., and Lisanti, M.P. (1996). Src Tyrosine Kinases, Gα Subunits, and H-Ras Share a Common Membrane-anchored Scaffolding Protein,

Caveolin binding negatively regulates the auto-activation of Src Tyrosine Kinases. J. Biol. Chem. *271*, 29182–29190.

Li, S., Okamoto, T., Chun, M., Sargiacomo, M., Casanova, J.E., Hansen, S.H., Nishimoto, I., and Lisanti, M.P. (1995). Evidence for a Regulated Interaction between Heterotrimeric G Proteins and Caveolin. J. Biol. Chem. *270*, 15693–15701.

Liu, Y., Casey, L., and Pike, L.J. (1998). Compartmentalization of Phosphatidylinositol 4,5-Bisphosphate in Low-Density Membrane Domains in the Absence of Caveolin. Biochemical and Biophysical Research Communications *245*, 684–690.

Ludwig, D.S., Tritos, N.A., Mastaitis, J.W., Kulkarni, R., Kokkotou, E., Elmquist, J., Lowell, B., Flier, J.S., and Maratos-Flier, E. (2001). Melanin-concentrating hormone overexpression in transgenic mice leads to obesity and insulin resistance. J. Clin. Invest. *107*, 379–386.

Luttrell, L.M., and Lefkowitz, R.J. (2002). The role of beta-arrestins in the termination and transduction of G-protein-coupled receptor signals. J. Cell. Sci. *115*, 455–465.

Macdonald, J.L., and Pike, L.J. (2005). A Simplified Method for the Preparation of Detergent-Free Lipid Rafts. J. Lipid Res. *46*, 1061–1067.

Marieb, E.N., and Hoehn, K. (2010). Human anatomy & physiology (San Francisco: Benjamin Cummings).

Marinissen, M.J., and Gutkind, J.S. (2001). G-protein-coupled receptors and signaling networks: emerging paradigms. Trends in Pharmacological Sciences *22*, 368–376.

Massol, R.H., Boll, W., Griffin, A.M., and Kirchhausen, T. (2006). A burst of auxilin recruitment determines the onset of clathrin-coated vesicle uncoating. Proc. Natl. Acad. Sci. U.S.A. *103*, 10265–10270.

Matveev, S.V., and Smart, E.J. (2002). Heterologous desensitization of EGF receptors and PDGF receptors by sequestration in caveolae. Am J Physiol Cell Physiol *282*, C935–C946.

Mayor, S., and Maxfield, F.R. (1995). Insolubility and redistribution of GPI-anchored proteins at the cell surface after detergent treatment. Mol. Biol. Cell *6*, 929–944.

Miyamoto-Matsubara, M., Chung, S., and Saito, Y. (2010). Functional interaction of regulator of G protein signaling-2 with melanin-concentrating hormone receptor 1. Ann. N. Y. Acad. Sci. *1200*, 112–119.

Moden, J. (2012). An Investigation of Melanin-concentrating Hormone Receptor Internalization – Or Lack Thereof. The College at Brockport State University of New York.

Monier, S., Parton, R.G., Vogel, F., Behlke, J., Henske, A., and Kurzchalia, T.V. (1995). VIP21-caveolin, a membrane protein constituent of the caveolar coat, oligomerizes in vivo and in vitro. Mol. Biol. Cell *6*, 911–927.

Mori, M., Harada, M., Terao, Y., Sugo, T., Watanabe, T., Shimomura, Y., Abe, M., Shintani, Y., Onda, H., Nishimura, O., et al. (2001). Cloning of a novel G protein-coupled receptor, SLT, a subtype of the melanin-concentrating hormone receptor. Biochem. Biophys. Res. Commun. *283*, 1013–1018.

Morrison, C.D., Morton, G.J., Niswender, K.D., Gelling, R.W., and Schwartz, M.W. (2005). Leptin inhibits hypothalamic Npy and Agrp gene expression via a mechanism that requires phosphatidylinositol 3-OH-kinase signaling. Am J Physiol Endocrinol Metab *289*, E1051–E1057.

Mosher, W.D., Jones, J., and National Center for Health Statistics (U.S.) (2010). Use of contraception in the United States: 1982-2008. (Hyattsville, Md.: U.S. Dept. of Health and Human Services, Centers for Disease Control and Prevention, National Center for Health Statistics).

Must, A. (1999). The Disease Burden Associated With Overweight and Obesity. JAMA: The Journal of the American Medical Association *282*, 1523–1529.

Naito, N., Nakai, Y., Kawauchi, H., and Hayashi, Y. (1985). Immunocytochemical identification of melanin-concentrating hormone in the brain and pituitary gland of the teleost fishes; Cell and Tissue Research *242*, 41–48.

Nichols, B. (2003). Caveosomes and endocytosis of lipid rafts. J. Cell. Sci. *116*, 4707–4714.

Oakley, R.H., Laporte, S.A., Holt, J.A., Barak, L.S., and Caron, M.G. (1999). Association of β-Arrestin with G Protein-coupled Receptors during Clathrin-mediated Endocytosis Dictates the Profile of Receptor Resensitization. J. Biol. Chem. *274*, 32248–32257.

Palade, G.E. (1953). An electron microscope study of the mitochondrial structure. J. Histochem. Cytochem. *1*, 188–211.

Parton, R.G. (1996). Caveolae and caveolins. Curr. Opin. Cell Biol. *8*, 542–548.

Parton, R.G., Joggerst, B., and Simons, K. (1994). Regulated internalization of caveolae. J. Cell Biol. *127*, 1199–1215.

Parton, R.G., and Simons, K. (2007). The multiple faces of caveolae. Nature Reviews Molecular Cell Biology *8*, 185–194.

Pasquali, R., Pelusi, C., Genghini, S., Cacciari, M., and Gambineri, A. (2003). Obesity and reproductive disorders in women. Hum. Reprod. Update *9*, 359–372.

Pearse, B.M. (1976). Clathrin: a unique protein associated with intracellular transfer of membrane by coated vesicles. Proc. Natl. Acad. Sci. U.S.A. *73*, 1255–1259.

Pelkmans, L., Kartenbeck, J., and Helenius, A. (2001). Caveolar endocytosis of simian virus 40 reveals a new two-step vesicular-transport pathway to the ER. Nat. Cell Biol. *3*, 473–483.

Pissios, P., Trombly, D.J., Tzameli, I., and Maratos-Flier, E. (2003). Melanin-concentrating hormone receptor 1 activates extracellular signal-regulated kinase and synergizes with G(s)-coupled pathways. Endocrinology *144*, 3514–3523.

Pol, A., Luetterforst, R., Lindsay, M., Heino, S., Ikonen, E., and Parton, R.G. (2001). A caveolin dominant negative mutant associates with lipid bodies and induces intracellular cholesterol imbalance. J. Cell Biol. *152*, 1057–1070.

Pol, A., Martin, S., Fernandez, M.A., Ferguson, C., Carozzi, A., Luetterforst, R., Enrich, C., and Parton, R.G. (2004). Dynamic and regulated association of caveolin with lipid bodies: modulation of lipid body motility and function by a dominant negative mutant. Mol. Biol. Cell *15*, 99–110.

Qu, D., Ludwig, D.S., Gammeltoft, S., Piper, M., Pelleymounter, M.A., Cullen, M.J., Mathes, W.F., Przypek, R., Kanarek, R., and Maratos-Flier, E. (1996). A role for melanin-concentrating hormone in the central regulation of feeding behaviour. Nature *380*, 243–247.

Qualmann, B., Roos, J., DiGregorio, P.J., and Kelly, R.B. (1999). Syndapin I, a synaptic dynamin-binding protein that associates with the neural Wiskott-Aldrich syndrome protein. Mol. Biol. Cell *10*, 501–513.

Rahmouni, K., Haynes, W.G., Morgan, D.A., and Mark, A.L. (2002). Selective Resistance to Central Neural Administration of Leptin in Agouti Obese Mice. Hypertension *39*, 486–490.

Rivera, R., Yacobson, I., and Grimes, D. (1999). The mechanism of action of hormonal contraceptives and intrauterine contraceptive devices. Am. J. Obstet. Gynecol. *181*, 1263–1269.

Rodriguez, M., Beauverger, P., Naime, I., Rique, H., Ouvry, C., Souchaud, S., Dromaint, S., Nagel, N., Suply, T., Audinot, V., et al. (2001). Cloning and molecular characterization of the novel human melanin-concentrating hormone receptor MCH2. Mol. Pharmacol. *60*, 632–639.

Roess, D.A., Horvat, R.D., Munnelly, H., and Barisas, B.G. (2000). Luteinizing hormone receptors are self-associated in the plasma membrane. Endocrinology *141*, 4518–4523.

Rosenbaum, D.M., Rasmussen, S.G.F., and Kobilka, B.K. (2009). The structure and function of G-protein-coupled receptors. Nature *459*, 356–363.

Roth, T.F., and Porter, K.R. (1964). Yolk Protein uptake in the oocyte of the mosquito Aedes Aegypti. L. J. Cell Biol. *20*, 313–332.

Saito, Y., Tetsuka, M., Li, Y., Kurose, H., and Maruyama, K. (2004). Properties of rat melanin-concentrating hormone receptor 1 internalization. Peptides *25*, 1597–1604.

Schlessinger, J. (2000). Cell signaling by receptor tyrosine kinases. Cell *103*, 211–225.

Shenoy, S.K., and Lefkowitz, R.J. (2003). Multifaceted roles of beta-arrestins in the regulation of seven-membrane-spanning receptor trafficking and signalling. Biochem J *375*, 503–515.

Shi, Y. (2004). Beyond skin color: emerging roles of melanin-concentrating hormone in energy homeostasis and other physiological functions. Peptides *25*, 1605–1611.

Sleer, L.S., Brown, A.J., and Stanley, K.K. (2001). Interaction of caveolin with 7-ketocholesterol. Atherosclerosis *159*, 49–55.

Smart, E.J., Graf, G.A., McNiven, M.A., Sessa, W.C., Engelman, J.A., Scherer, P.E., Okamoto, T., and Lisanti, M.P. (1999). Caveolins, liquid-ordered domains, and signal transduction. Mol. Cell. Biol. *19*, 7289–7304.

Smart, E.J., Ying, Y.S., Mineo, C., and Anderson, R.G. (1995). A detergent-free method for purifying caveolae membrane from tissue culture cells. Proc. Natl. Acad. Sci. U.S.A. *92*, 10104–10108.

Song, K.S., Li, S., Okamoto, T., Quilliam, L.A., Sargiacomo, M., and Lisanti, M.P. (1996). Co-purification and Direct Interaction of Ras with Caveolin, an Integral Membrane Protein of Caveolae Microdomains detergent free isolation of Caveolae. J. Biol. Chem. *271*, 9690–9697.

Stenmark, H., Vitale, G., Ullrich, O., and Zerial, M. (1995). Rabaptin-5 is a direct effector of the small GTPase Rab5 in endocytic membrane fusion. Cell *83*, 423–432.

Takekawa, S., Asami, A., Ishihara, Y., Terauchi, J., Kato, K., Shimomura, Y., Mori, M., Murakoshi, H., Kato, K., Suzuki, N., et al. (2002). T-226296: a novel, orally active and selective melanin-concentrating hormone receptor antagonist. Eur. J. Pharmacol. *438*, 129–135.

Tan, C.P., Sano, H., Iwaasa, H., Pan, J., Sailer, A.W., Hreniuk, D.L., Feighner, S.D., Palyha, O.C., Pong, S.-S., Figueroa, D.J., et al. (2002). Melanin-concentrating hormone receptor subtypes 1 and 2: species-specific gene expression. Genomics *79*, 785–792.

Tang, Z., Scherer, P.E., Okamoto, T., Song, K., Chu, C., Kohtz, D.S., Nishimoto, I., Lodish, H.F., and Lisanti, M.P. (1996). Molecular Cloning of Caveolin-3, a Novel Member of the Caveolin Gene Family Expressed Predominantly in Muscle. J. Biol. Chem. *271*, 2255–2261.

Tetsuka, M., Saito, Y., Imai, K., Doi, H., and Maruyama, K. (2004). The basic residues in the membrane-proximal C-terminal tail of the rat melanin-concentrating hormone receptor 1 are required for receptor function. Endocrinology *145*, 3712–3723.

Thomsen, P., Roepstorff, K., Stahlhut, M., and Deurs, B. van (2002). Caveolae Are Highly Immobile Plasma Membrane Microdomains, Which Are not Involved in Constitutive Endocytic Trafficking. Mol. Biol. Cell *13*, 238–250.

Traub, L.M. (2003). Sorting it out: AP-2 and alternate clathrin adaptors in endocytic cargo selection. J. Cell Biol. *163*, 203–208.

Tritos, N.A., Mastaitis, J.W., Kokkotou, E., and Maratos-Flier, E. (2001). Characterization of melanin concentrating hormone and preproorexin expression in the murine hypothalamus. Brain Research *895*, 160–166.

Tritos, N.A., Vicent, D., Gillette, J., Ludwig, D.S., Flier, E.S., and Maratos-Flier, E. (1998). Functional interactions between melanin-concentrating hormone,

neuropeptide Y, and anorectic neuropeptides in the rat hypothalamus. Diabetes *47*, 1687–1692.

De Vries, L., Zheng, B., Fischer, T., Elenko, E., and Farquhar, M.G. (2000). The regulator of G protein signaling family. Annu. Rev. Pharmacol. Toxicol. *40*, 235–271.

Wang, H., Storlien, L.H., and Huang, X.-F. (2002). Effects of dietary fat types on body fatness, leptin, and ARC leptin receptor, NPY, and AgRP mRNA expression. Am J Physiol Endocrinol Metab *282*, E1352–E1359.

Weiss, A., and Schlessinger, J. (1998). Switching signals on or off by receptor dimerization. Cell *94*, 277–280.

Wintermantel, T.M., Campbell, R.E., Porteous, R., Bock, D., Gröne, H.-J., Todman, M.G., Korach, K.S., Greiner, E., Pérez, C.A., Schütz, G., et al. (2006). Definition of Estrogen Receptor Pathway Critical for Estrogen Positive Feedback to Gonadotropin-Releasing Hormone Neurons and Fertility. Neuron *52*, 271–280.

Wolff, N.A., Lee, W.-K., and Thévenod, F. (2011). Role of Arf1 in endosomal trafficking of protein–metal complexes and cadmium–metallothionein-1 toxicity in kidney proximal tubule cells. Toxicology Letters *203*, 210–218.

Zhang, Y., Proenca, R., Maffei, M., Barone, M., Leopold, L., and Friedman, J.M. (1994). Positional cloning of the mouse obese gene and its human homologue. Nature *372*, 425–432.